

# 2D and 3D Kinetic Simulations of the MRX Reconnection Experiment

V. Roytershteyn, W. Daughton, L. Yin,  
B.J. Albright, K.J. Bowers

LANL

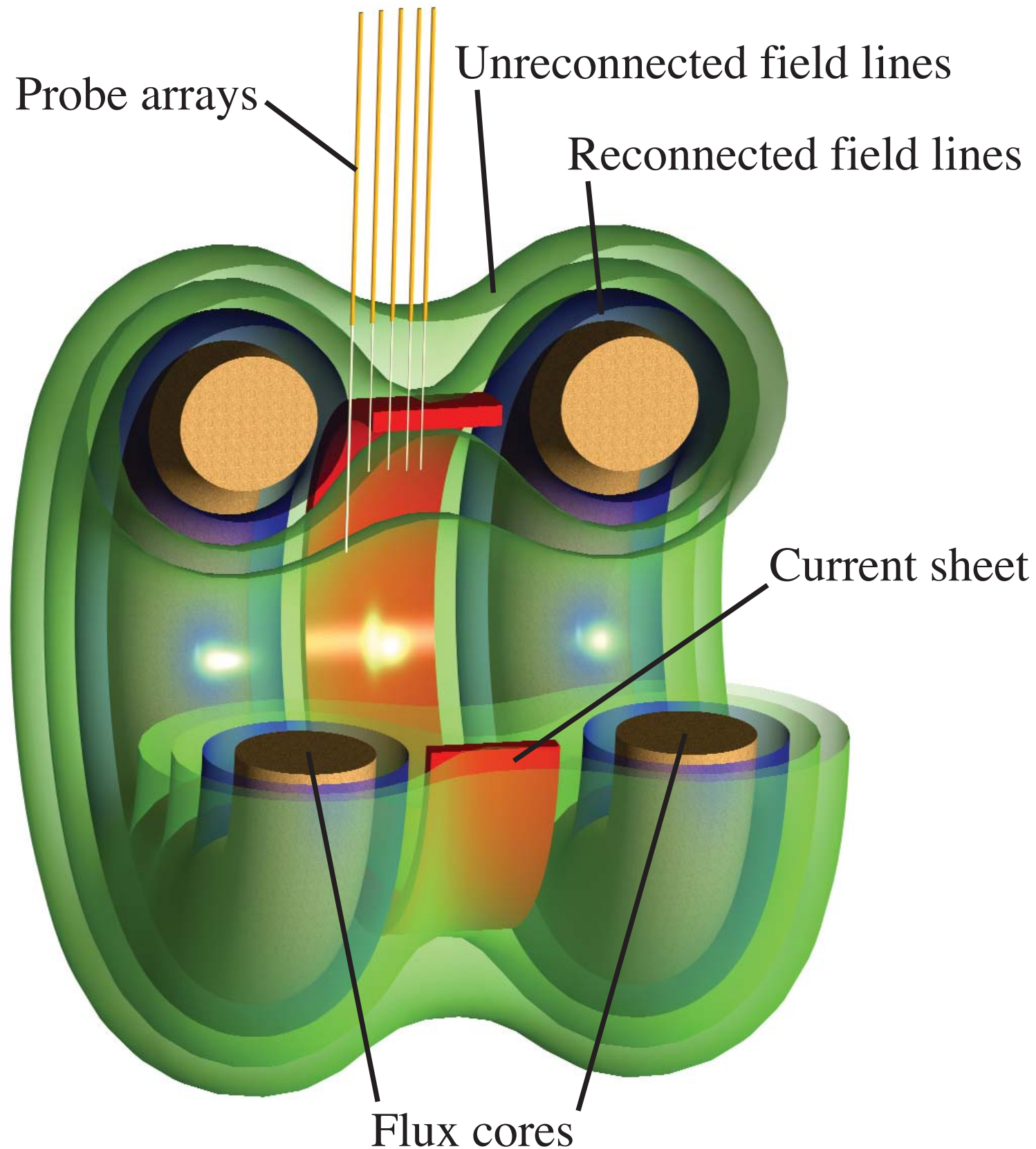
S. Dorfman, H. Ji, M. Yamada

PPPL

H. Karimabadi

UCSD

# The **M**agnetic **R**econnection **eX**periment - **MRX**



- Size  $\sim (150 \times 150) \text{ cm}$
- $T_e \sim 5 \text{ eV}$
- $n = (1-10) \cdot 10^{13} \text{ cm}^{-3}$
- electron m.f.p.  $\sim (0.5-5) \text{ cm}$
- layer width  $\sim 1 \text{ cm}$
- $d_i \sim 5 \text{ cm}$ ;

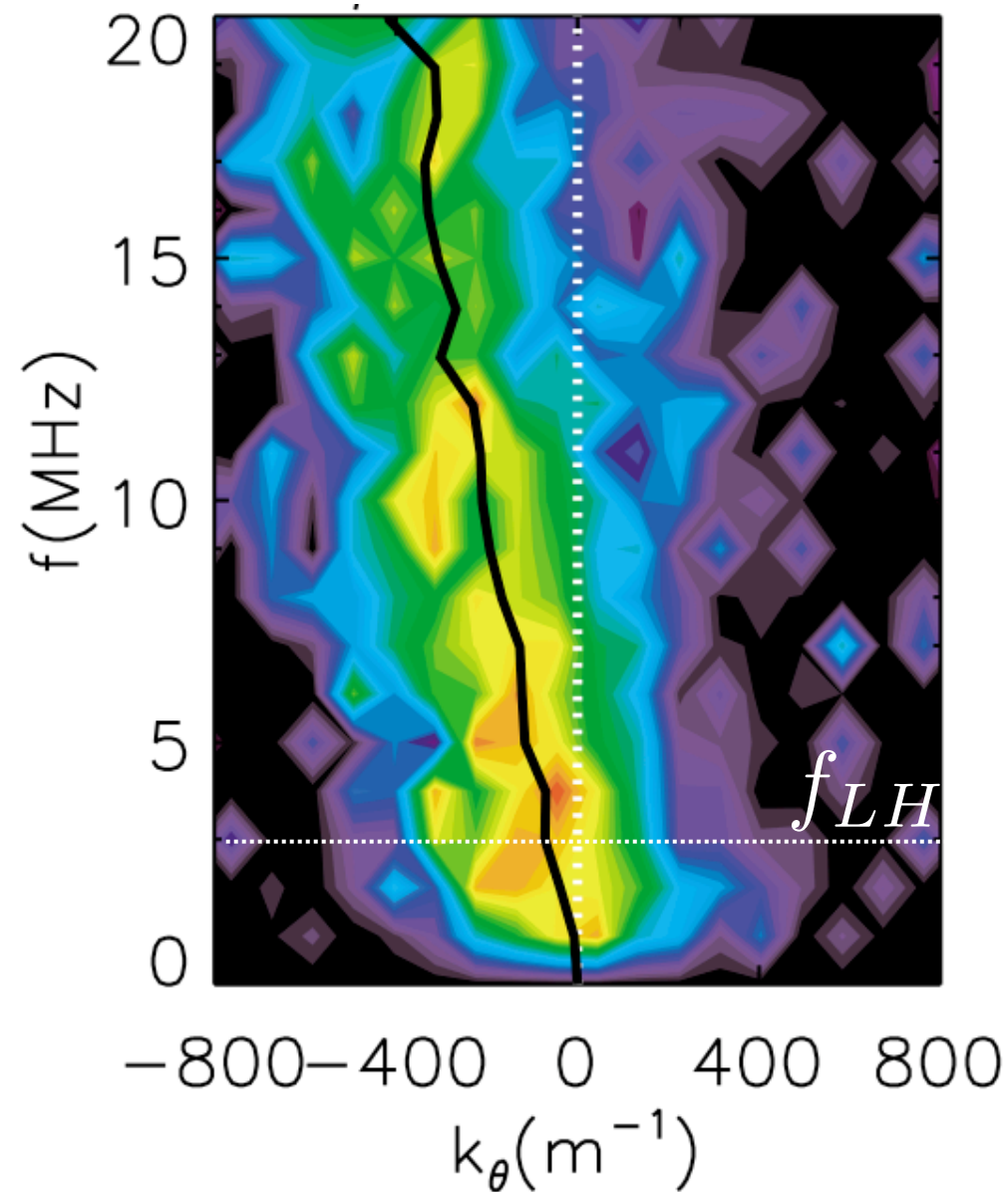
# Motivation

Can we better understand the structure of the diffusion region & the role of instabilities on reconnection?

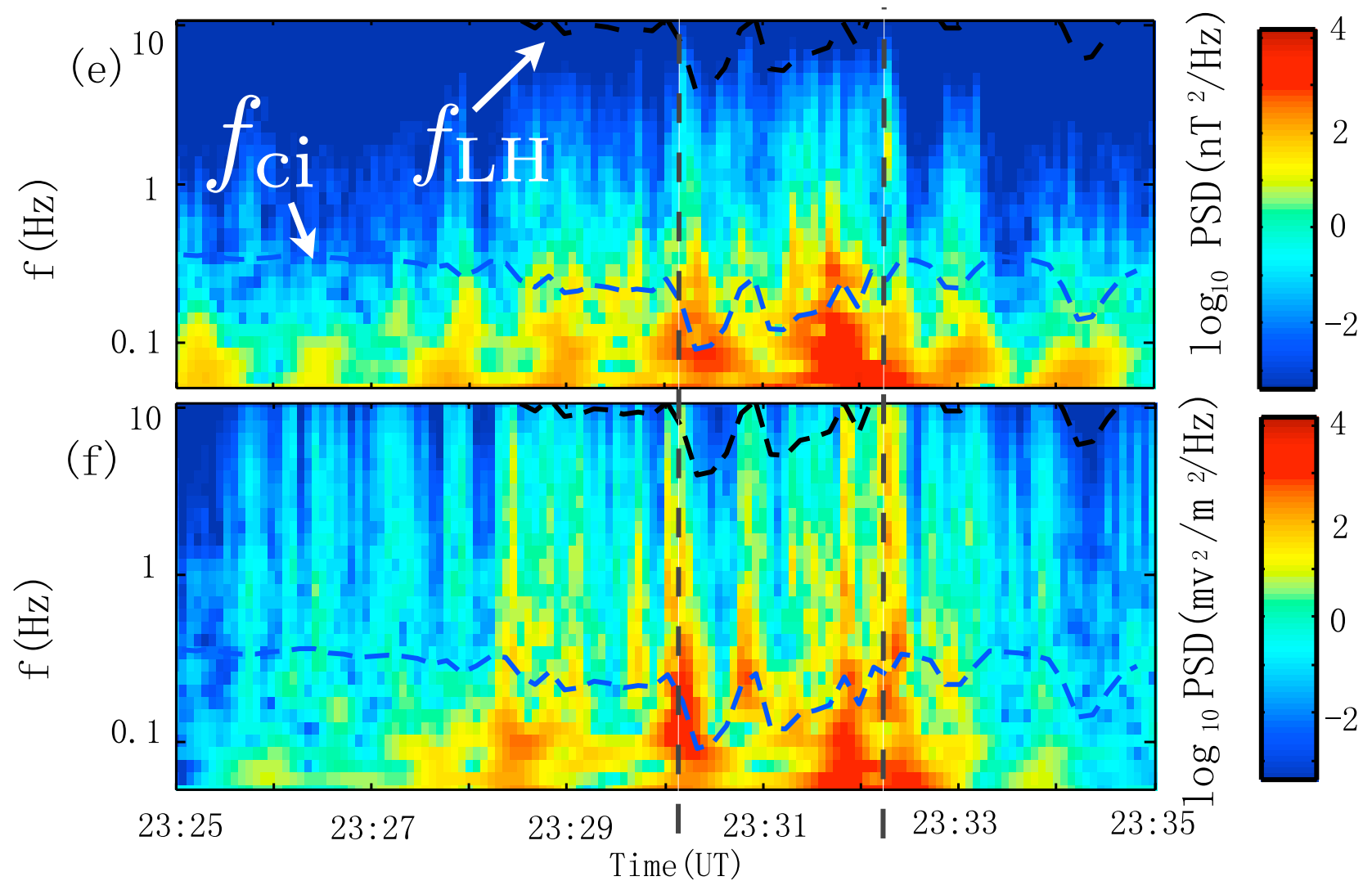
- Why use fully kinetic simulations?
  - Very weak guide field, complicated orbits
  - Near Dreicer limit  $E_R \lesssim E_{\text{crit}} \approx (m_e T_e)^{1/2} \nu_e / e$
  - Instabilities of interest are in the lower-hybrid range and can involve both ion & electron kinetic effects
- Broader goal - physics may also be relevant to reconnection in the Earth's magnetosphere
- By benchmarking kinetic simulations, we can more confidently extrapolate from laboratory to space parameters

# Electromagnetic instabilities in the lower-hybrid range are observed in both MRX and in the magnetosphere

Magnetic fluctuation at the MRX layer center (Ji *et al.*, PRL 04)



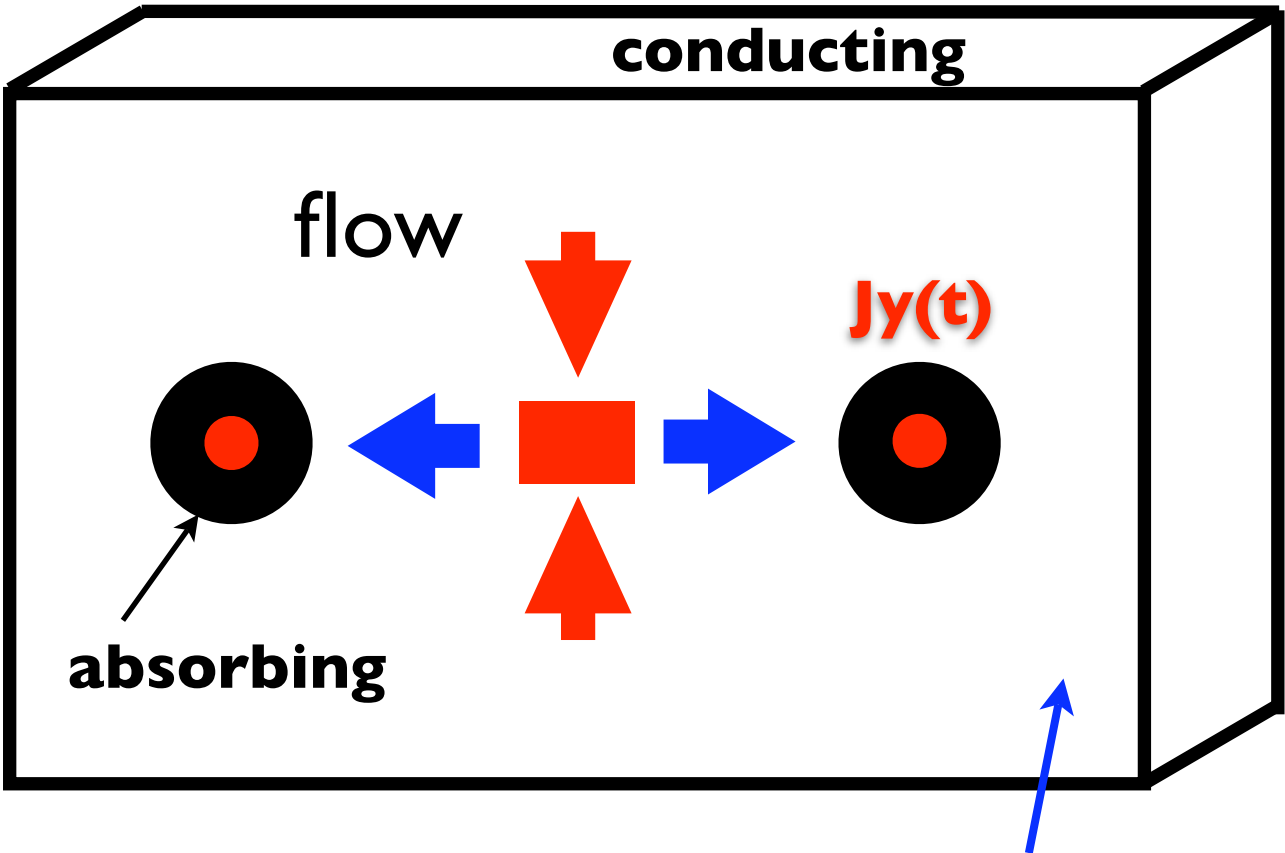
Cluster observations in the tail (Zhou, *et al.*, GRL, 2009)



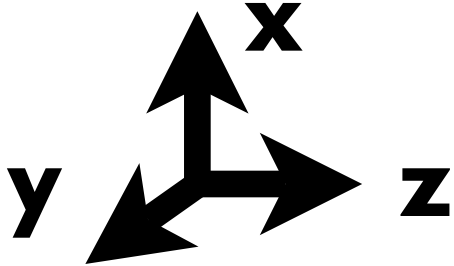
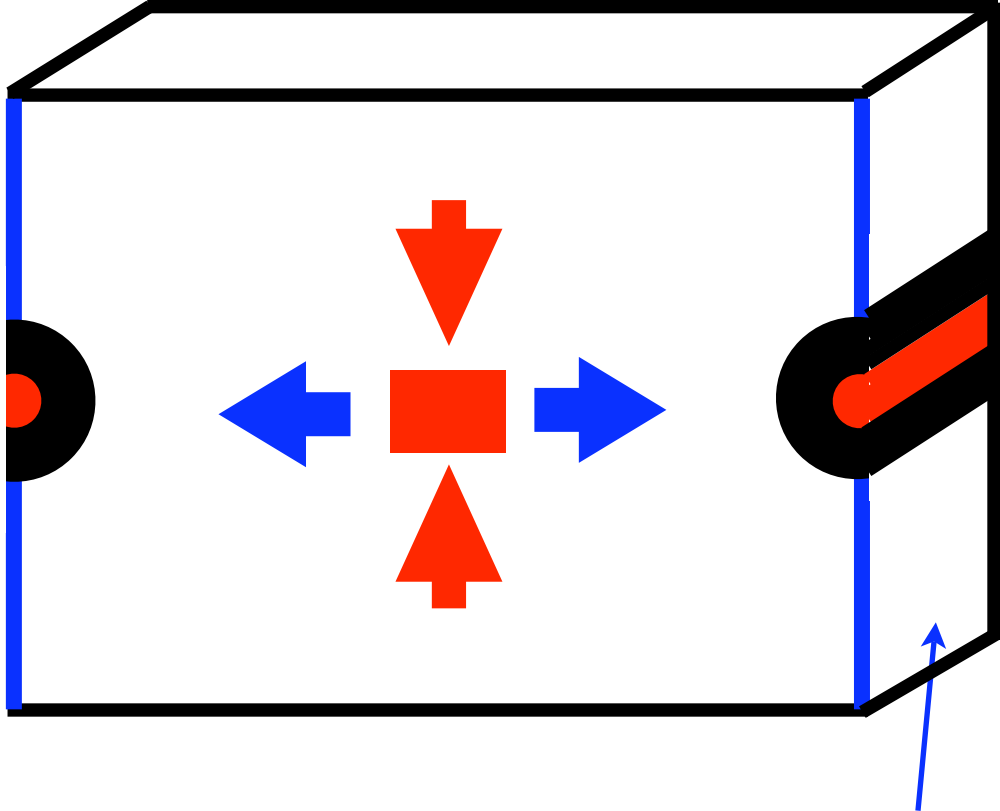
# Simulation Geometry

Slab geometry (short-wavelength modes)

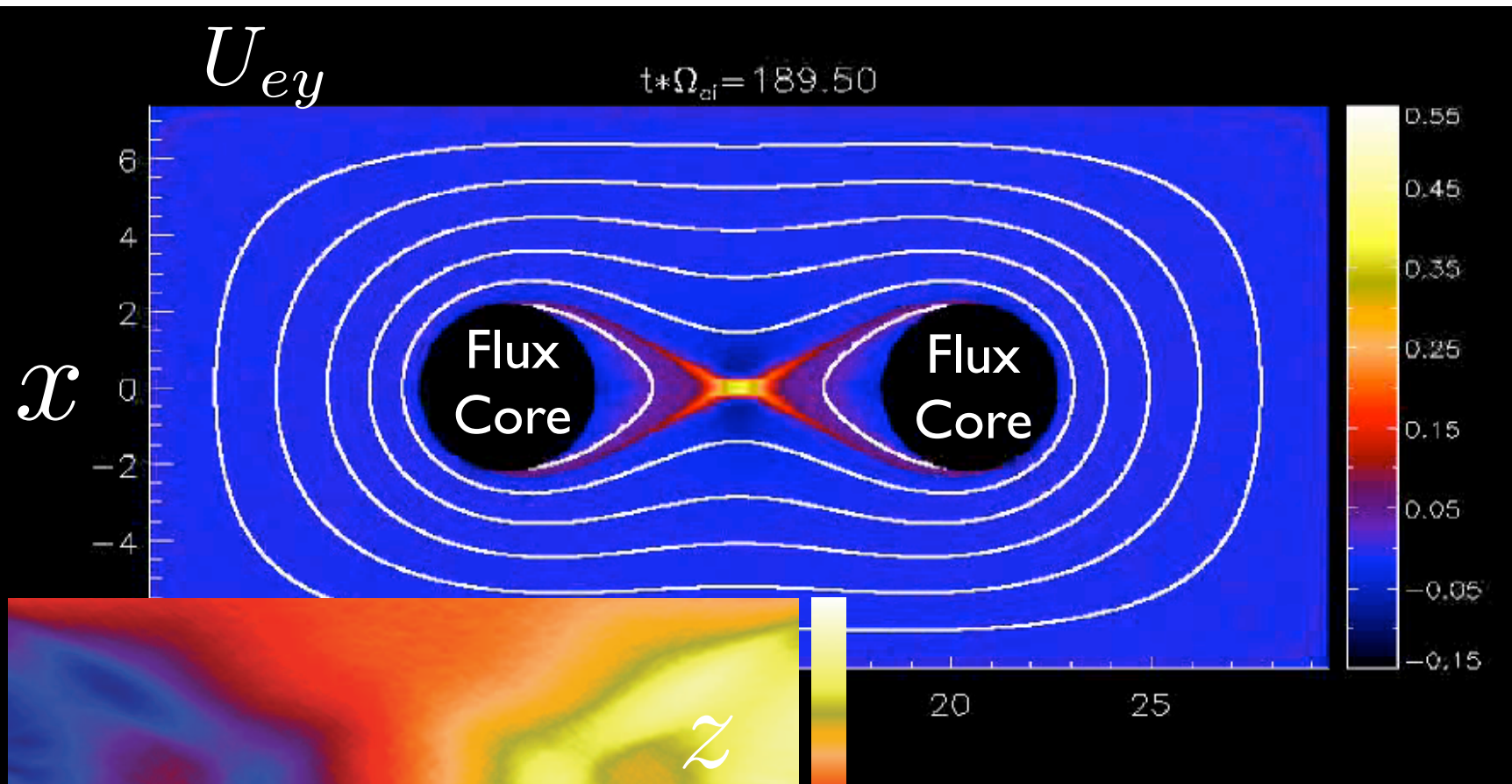
Mostly used in 2D



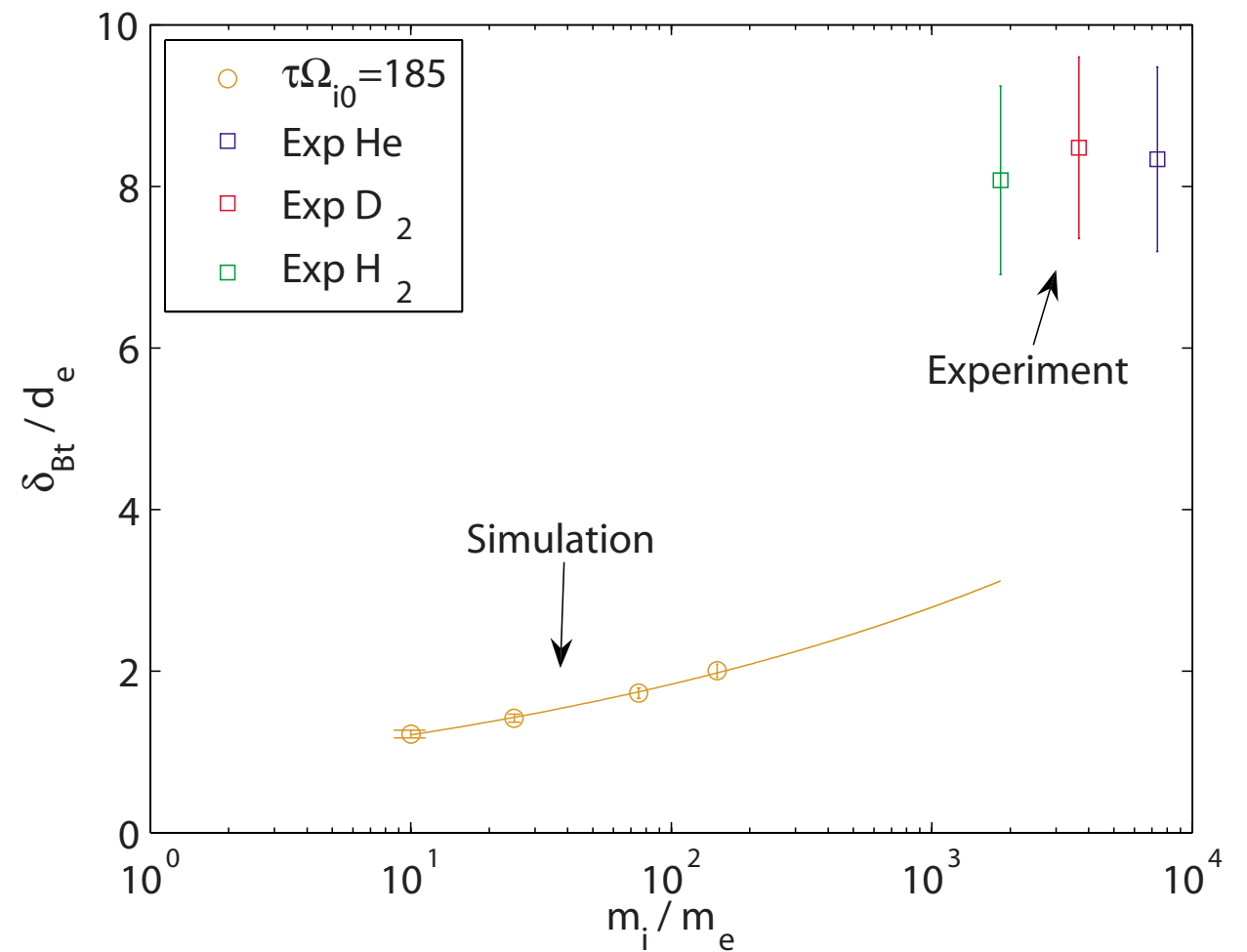
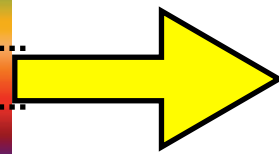
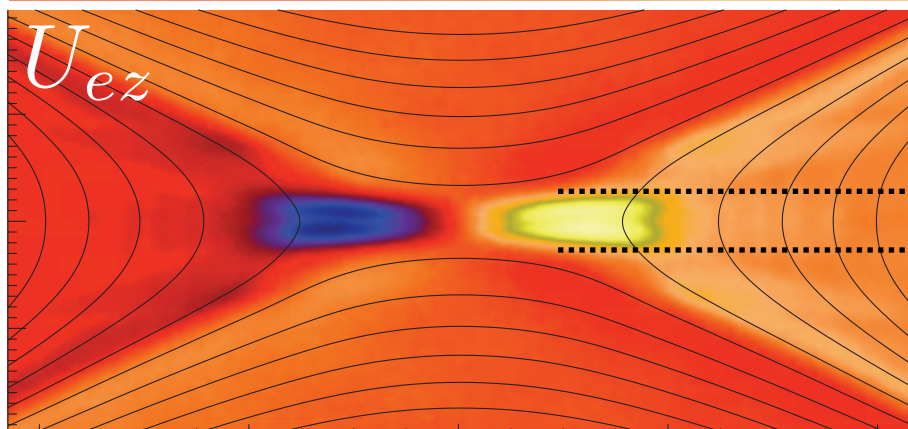
Used in 3D



# First started in 2D collisionless limit

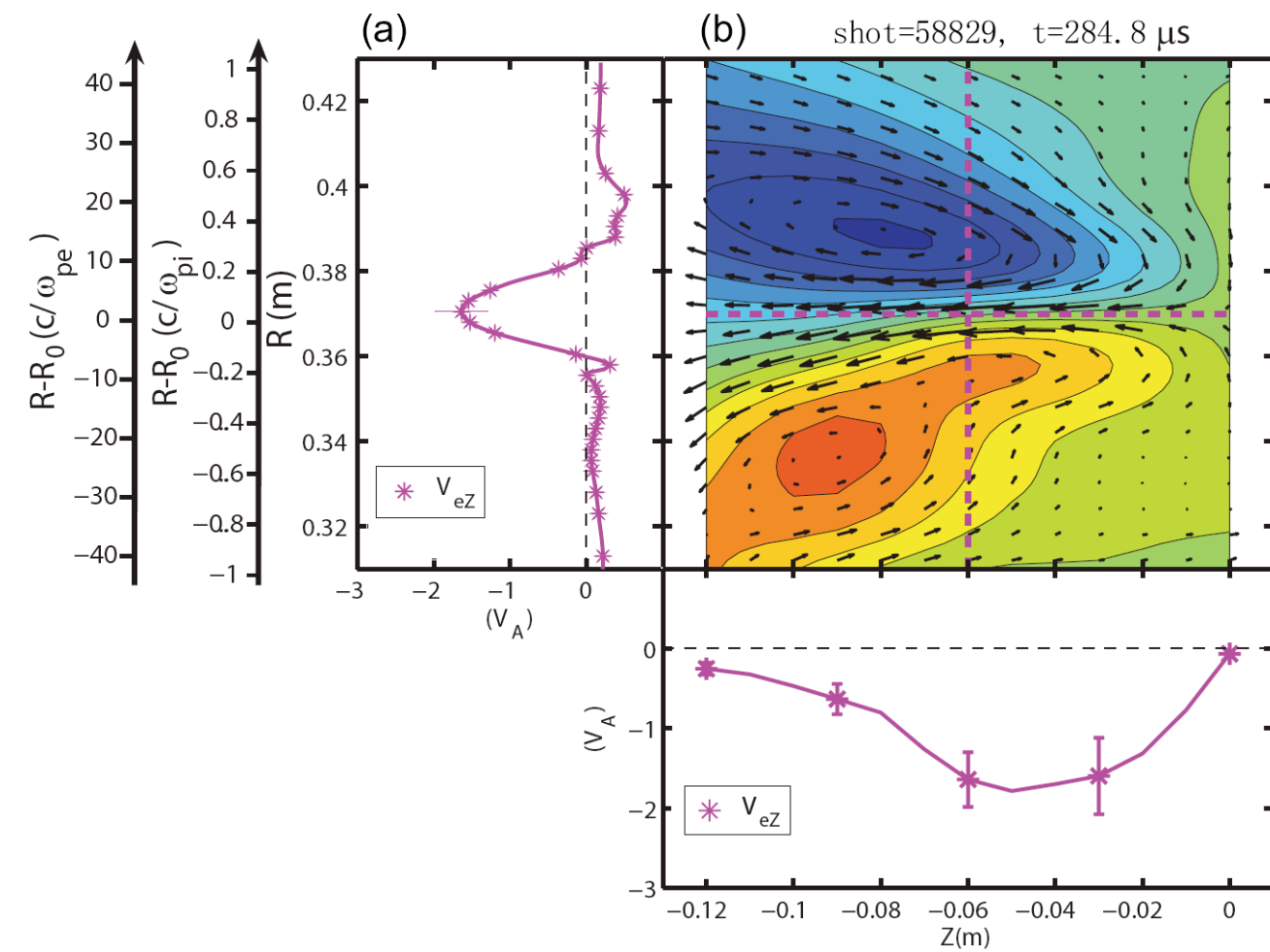


Dorfman et al,  
PoP 2008

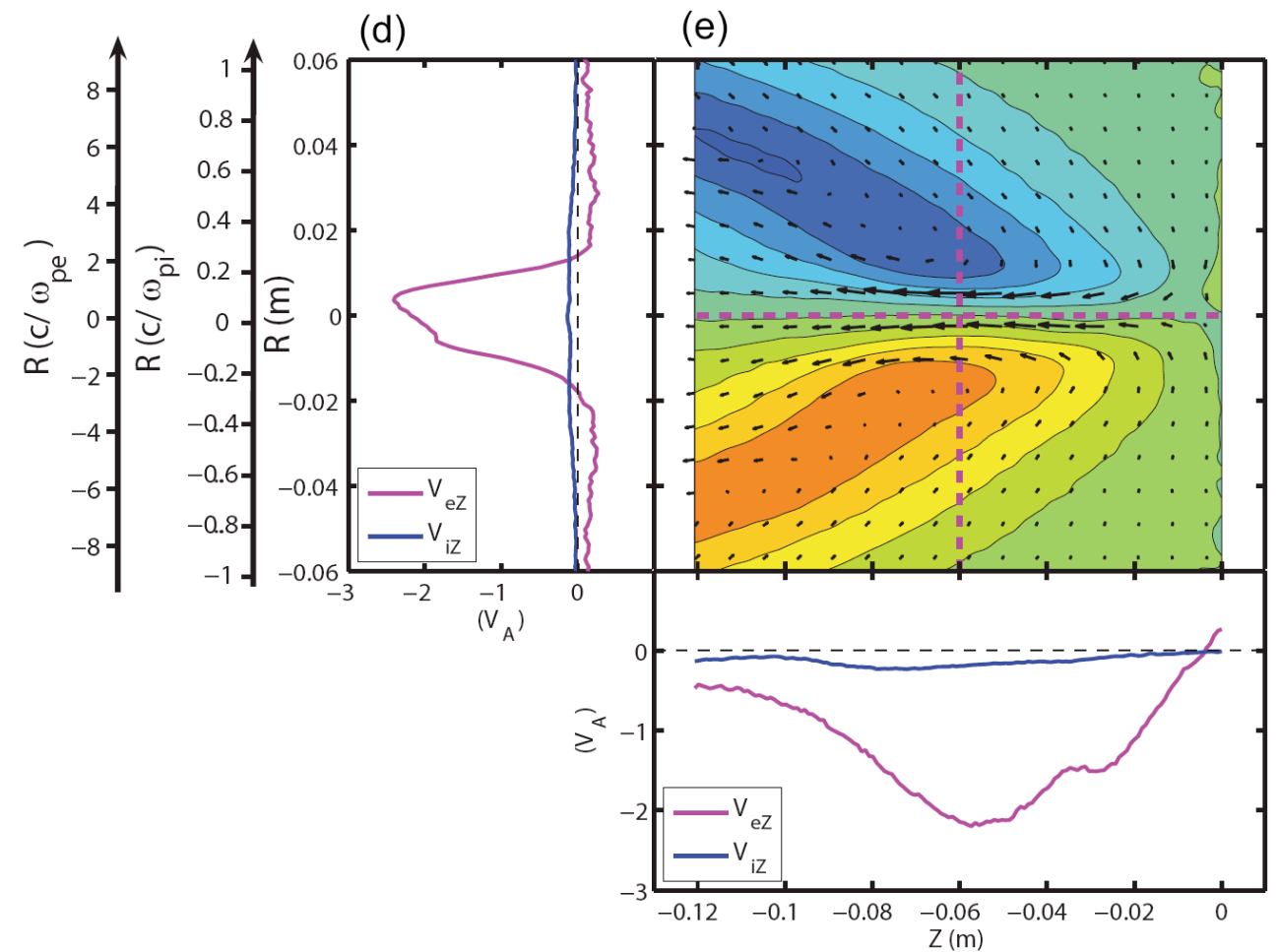


# 2D simulations reproduce the ion-scale current sheet structure

## Experiment



## 2D collisionless PIC



# Discrepancy motivated need for 3D + collisions

3D, high-performance explicit electromagnetic code VPIC  
(K. Bowers) + collision model

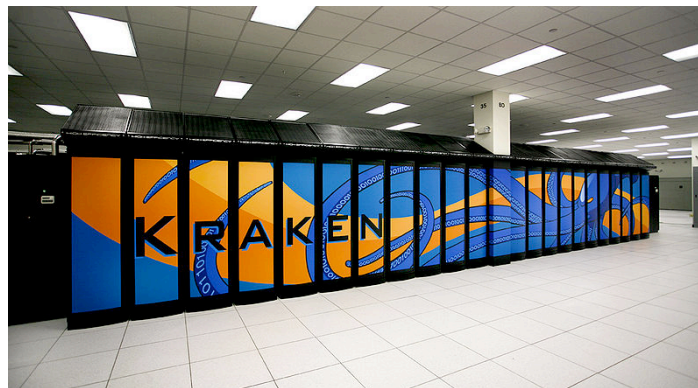
$$\frac{\partial f_s}{\partial t} + \mathbf{v} \cdot \nabla f_s + \frac{q_s}{m_s} \left( \mathbf{E} + \frac{1}{c} \mathbf{v} \times \mathbf{B} \right) \cdot \nabla_{\mathbf{v}} f_s = \sum_{s'} \mathcal{C}\{f_s, f_{s'}\}$$

+ Maxwell's equations

The code runs on a variety of peta-scale machines.  
Largest simulation to date: over a *trillion* particles



Roadrunner  
(LANL)



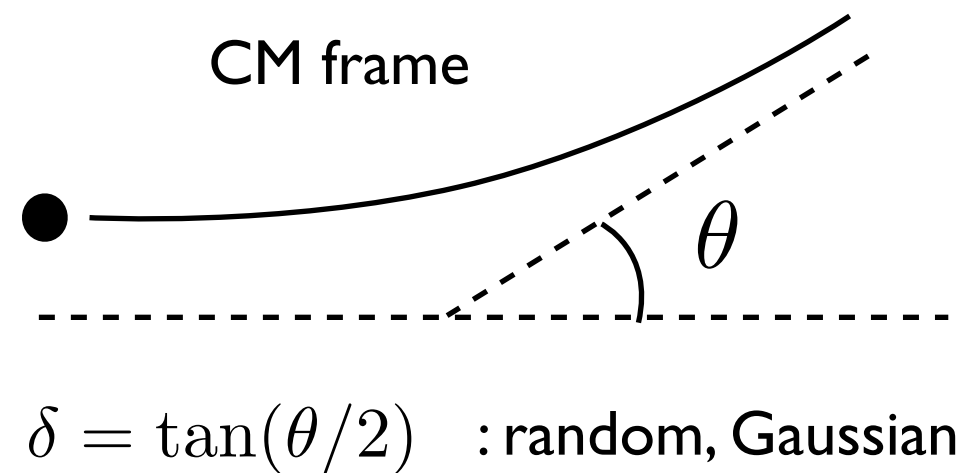
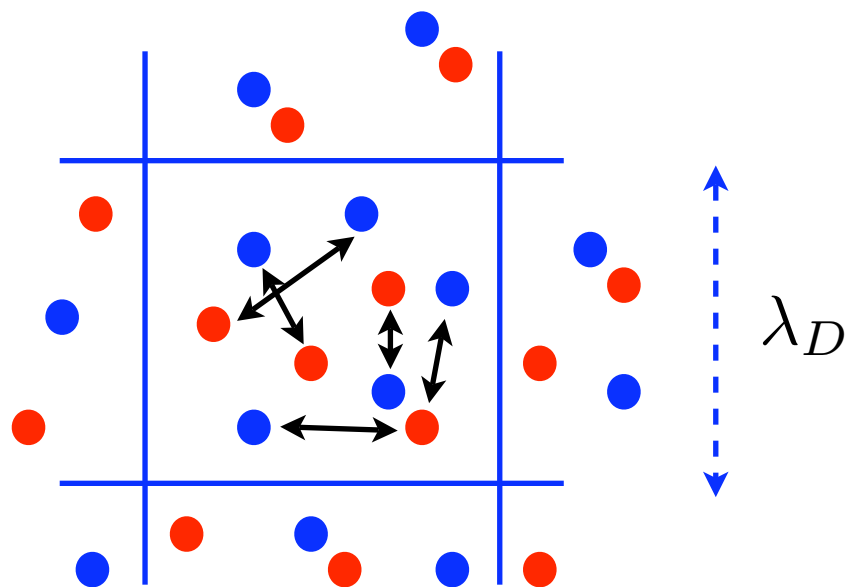
Kraken  
NICS/NSF



Jaguar  
ORNL

# Takizuka-Abe particle-pairing algorithm: expensive, but accurate

- converges to Landau collision integral
- conserves momentum and energy in each collision



$$\langle \delta^2 \rangle = \frac{2\pi e^4 n_s \ln \Lambda}{m_{s'}^2 |\mathbf{v}_s - \mathbf{v}'_s|^3} \Delta t_{\text{col}}$$

$$\mathcal{C}\{f_s, f_{s'}\} \rightarrow \frac{2\pi e^4 \ln \Lambda}{m_s} \nabla_v \cdot \int d^3v \frac{u^2 \mathbf{I} - \mathbf{u}\mathbf{u}}{u^3} \cdot \left( \frac{f_{s'}}{m_{s'}} \nabla_v f - \frac{f}{m_s} \nabla_{v'} f_{s'} \right)$$

The collision model has been benchmarked on a variety of problems: W. Daughton *et al.*, *Phys. Plasmas* **16**, p. 072111 (2009); D. Lemons *et al.*, *J. Comp. Phys.*, **228**, p. 1391 (2009)

# Choice of the scaling approach is crucial

---

Not possible to match same dimensionless parameters as MRX.  
It is crucial to re-scale the problem in dimensionless form.

Our choice: reference values of

$$\beta \quad \tau \Omega_{ci} \quad L/d_i$$

are close to experiment

$$m_i/m_e, \omega_{pe}/\omega_{ce}$$

are treated as numerical parameters. Typical values:  
(100-400) and (2-5) respectively

$$d_i = c/\omega_{pi} \quad L : \text{system size} \quad \tau : \text{time scale for the coil current ramp-down}$$

# Several scaling choices are possible for the collision frequency scaling

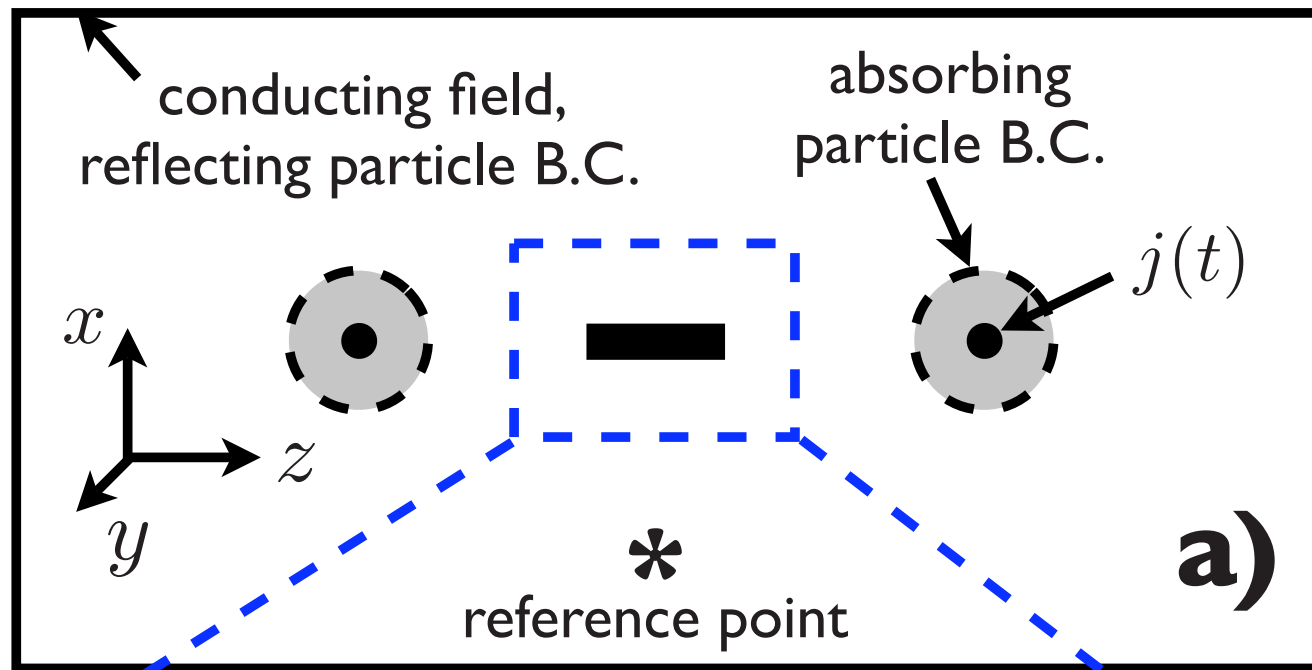
---

1) Match  $\nu_{ei}/\Omega_{ce}$  (representative range for MRX: 0.01-0.1)

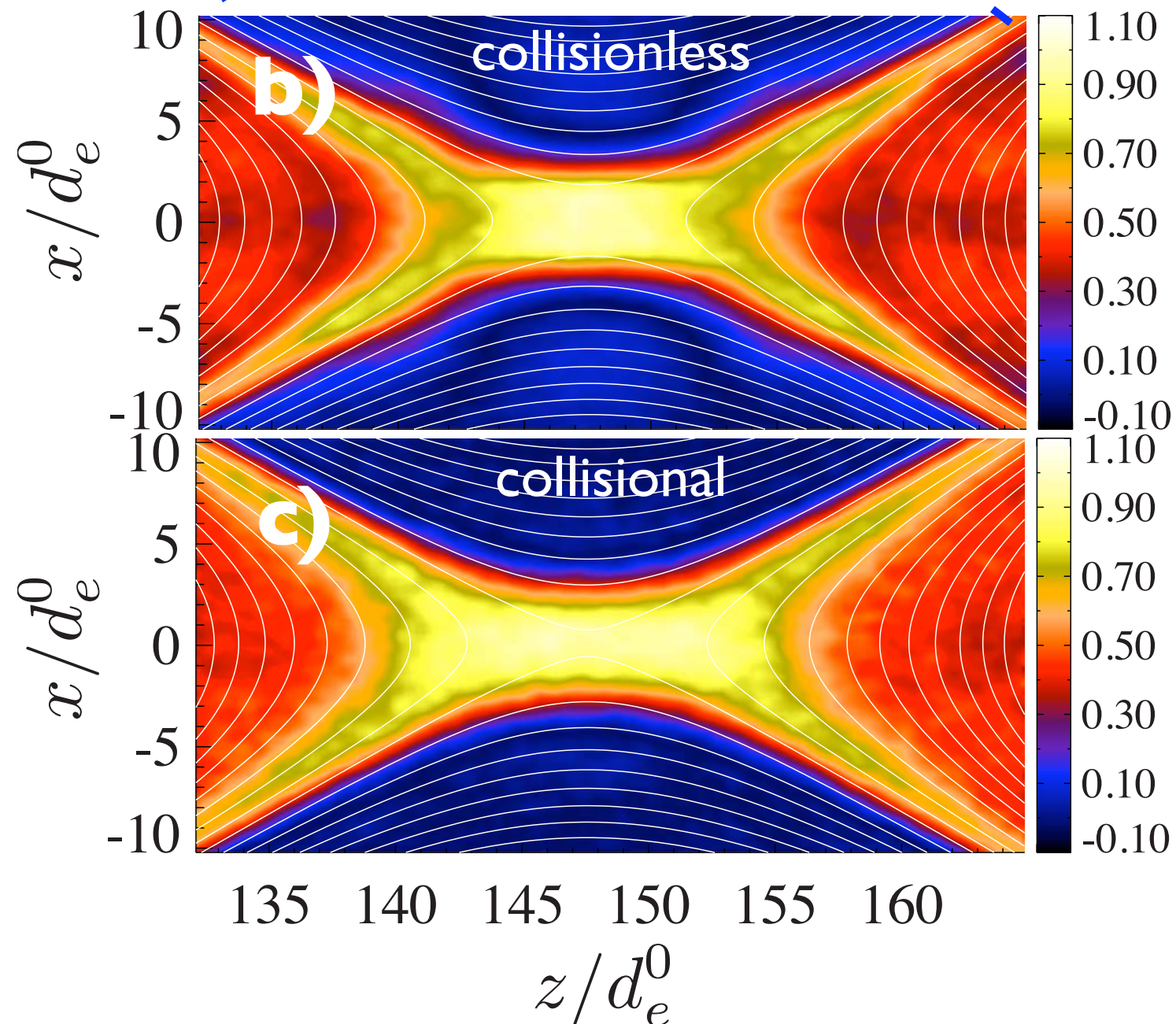
Appropriate for resistive regimes since it ensures matching of

$$S = \frac{LV_A}{D_m} \propto \frac{L}{d_i} \frac{\Omega_{ce}}{\nu_{ei}} \quad \frac{\delta_{SP}^2}{d_i^2} \propto \frac{L}{d_i} \frac{\nu_{ei}}{\Omega_{ce}}$$

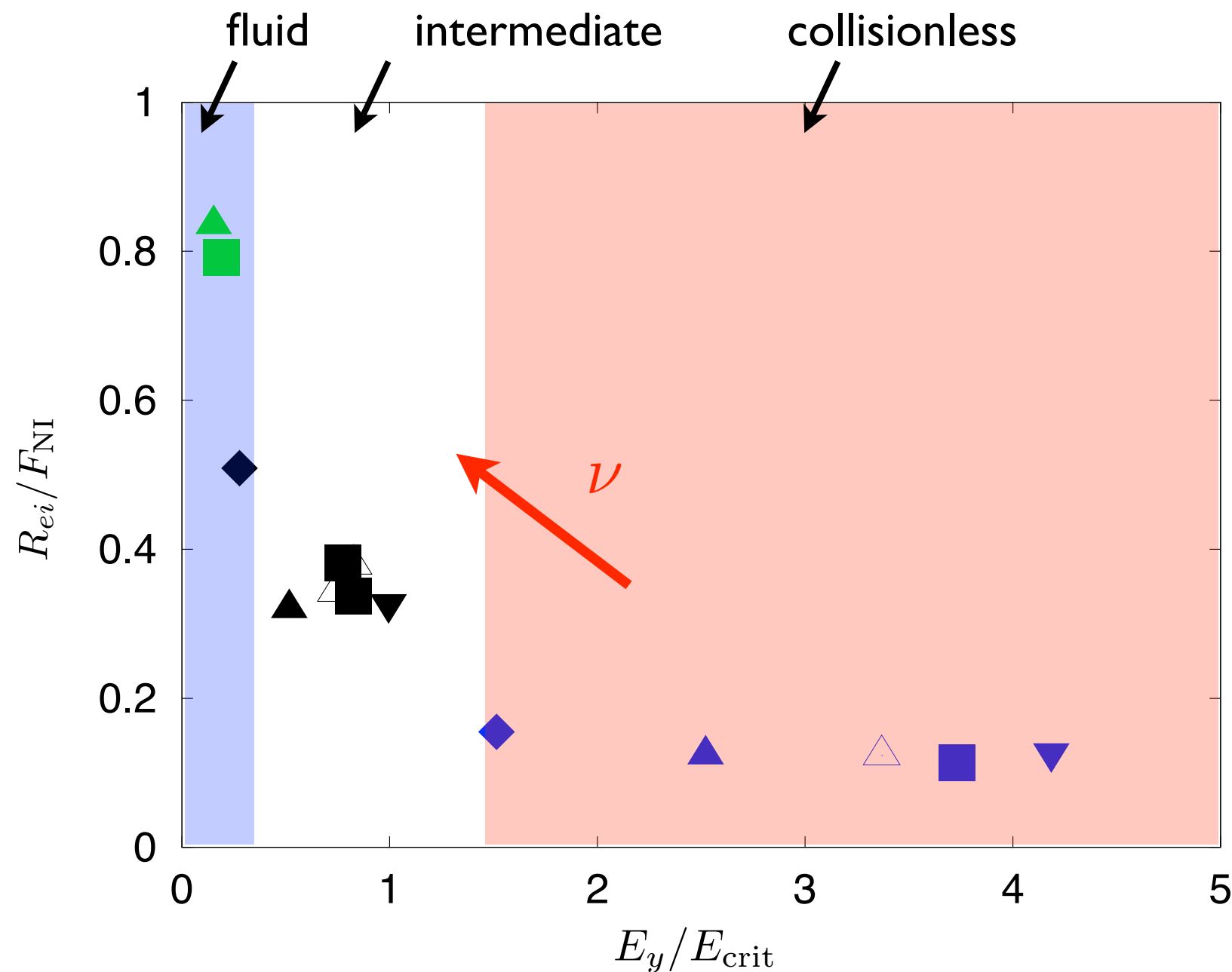
2) Match the ratio between reconnection electric field and the Drieger field (representative range of the experiment: 0.1-0.5). The relevant choice in 2D weakly collisional regimes



Roytershteyn et al,  
PoP, 2010



$$\underbrace{ne \left( \mathbf{E} + \frac{1}{c} \mathbf{v} \times \mathbf{B} \right)}_{F_{\text{NI}}} = -\nabla \cdot \mathbf{P} + \mathbf{R}_{ei} - m_e n \frac{d\mathbf{U}_e}{dt}$$



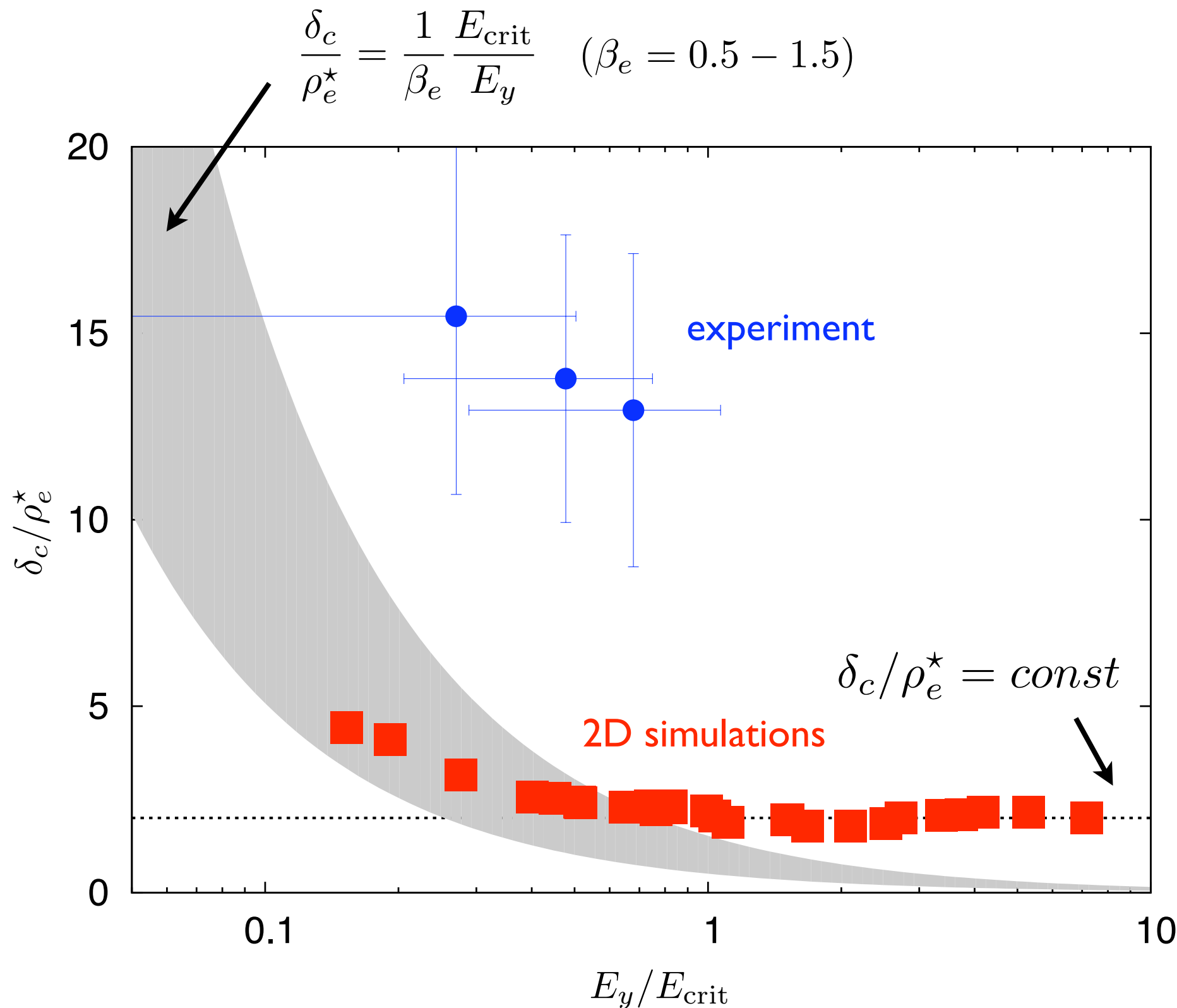
$$R_{ei,y} = \int d^3v v_y C_{ei} \{f_e, f_i\}$$

$$E_{\text{crit}} = \frac{\sqrt{2T_e m_e}}{e} \nu_{ei}$$

$$\nu_e = \frac{4\sqrt{2\pi} \Lambda n e^4}{3m_e^{1/2} T_e^{3/2}}$$

$$T_e = (\text{tr } \mathbf{P}_e) / (3n_e)$$

# The electron layer width (related to the reconnection mechanism) is systematically smaller in simulations



Simple limits:

collisionless

$$\delta / \rho_e^* = const$$

resistive

$$E = \eta_{\text{Spitzer}} j$$



$$\frac{\delta_c}{\rho_e^*} = \frac{1}{\beta_e} \frac{E_{\text{crit}}}{E_y}$$

# The origin of the large discrepancy is not understood

---

Clearly, effects beyond those present in 2D kinetic simulations are responsible for the observed layer width

Among the possible candidates

- 1) 3D instabilities/turbulence
- 2) Influence of neutrals and ionization processes
- 3) Broadening due to the probes

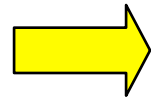
all of these possibilities can be addressed by simulations. some of the work is being carried out

# Influence of Lower-hybrid drift instability (LHDI)

## 2D Harris sheet

# Properties Depend on Sheet Thickness

**Regardless  
of  
Thickness**



1. Fastest growing modes  $\rightarrow k_y \rho_e \sim 1$
2. Both electrostatic and electromagnetic fluctuations
3. Broad range of unstable modes

**Thicker Sheets**  $\frac{\rho_i}{L} \leq 1$

Both ES and EM fluctuations are confined to the edge region for all wavelengths

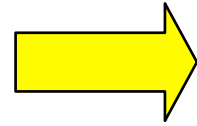
**Very Thin Sheets**  $\frac{\rho_i}{L} > 1.5$

Longer wavelength EM fluctuations are localized about center of the sheet while ES fluctuations remain confined to edge

Characteristic Wavelength  $\rightarrow k_y \sqrt{\rho_e \rho_i} \sim 1$

# Linear Theory of Thin Current Sheets

Linear Vlasov for ions and electrons



$$\frac{d\hat{f}_s}{dt} + \frac{q_s}{m_s} \left( \hat{\mathbf{E}} + \frac{\mathbf{v} \times \hat{\mathbf{B}}}{c} \right) \cdot \frac{\partial f_{os}}{\partial \mathbf{v}} = 0$$

Work with the Potentials:

$$\hat{\mathbf{E}} = -\nabla\phi - \frac{1}{c} \frac{\partial \hat{\mathbf{A}}}{\partial t}$$

$$\hat{\mathbf{B}} = \nabla \times \hat{\mathbf{A}}$$

Perturbations of the form:

$$\hat{\mathbf{A}} = \tilde{\mathbf{A}}(x) \exp[-i\omega t + ik_y y + ik_z z]$$

$$\hat{\phi} = \tilde{\phi}(x) \exp[-i\omega t + ik_y y + ik_z z]$$

Maxwell's Equations:

Lorentz Gauge

$$\nabla \cdot \hat{\mathbf{A}} + \frac{1}{c} \frac{\partial \hat{\phi}}{\partial t} = 0$$

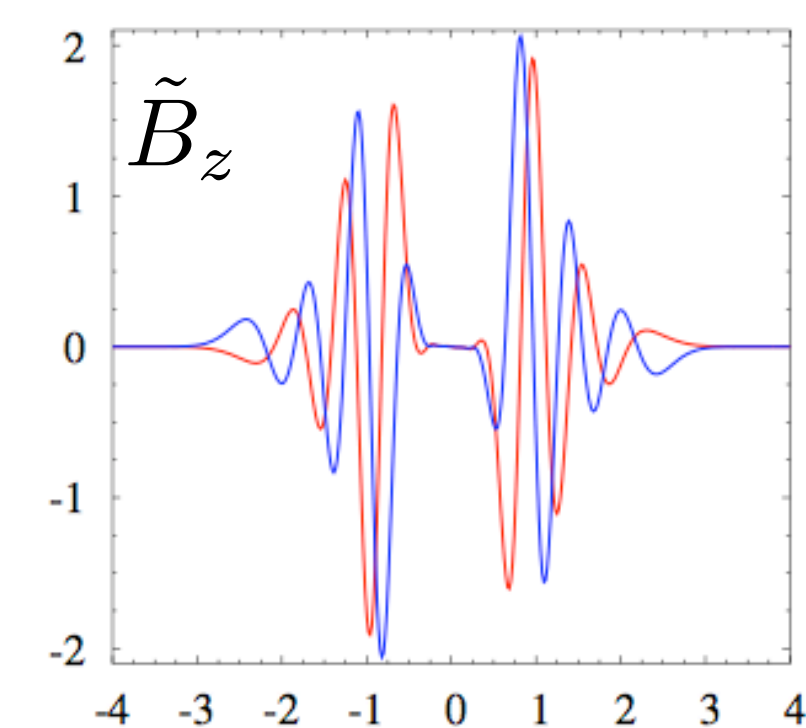
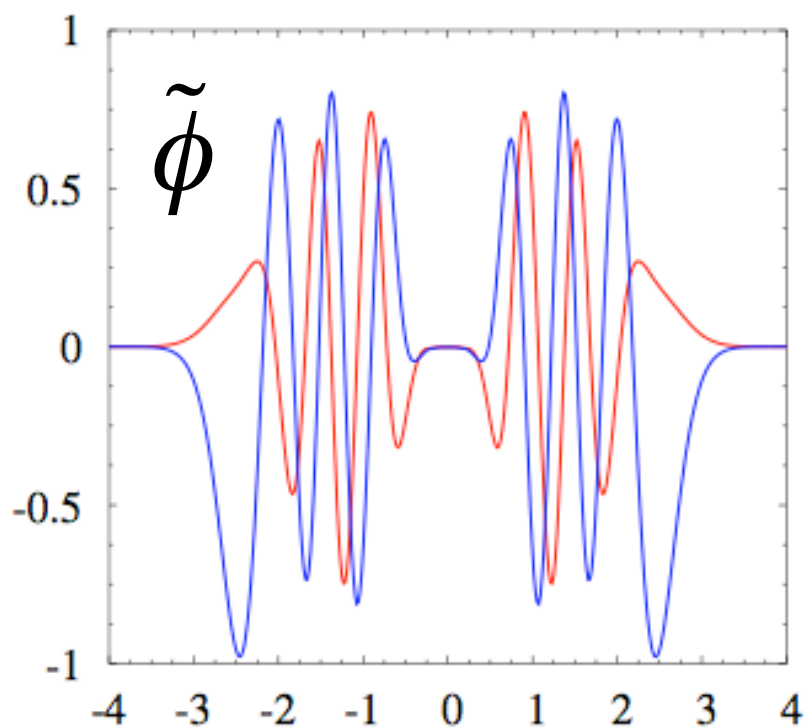
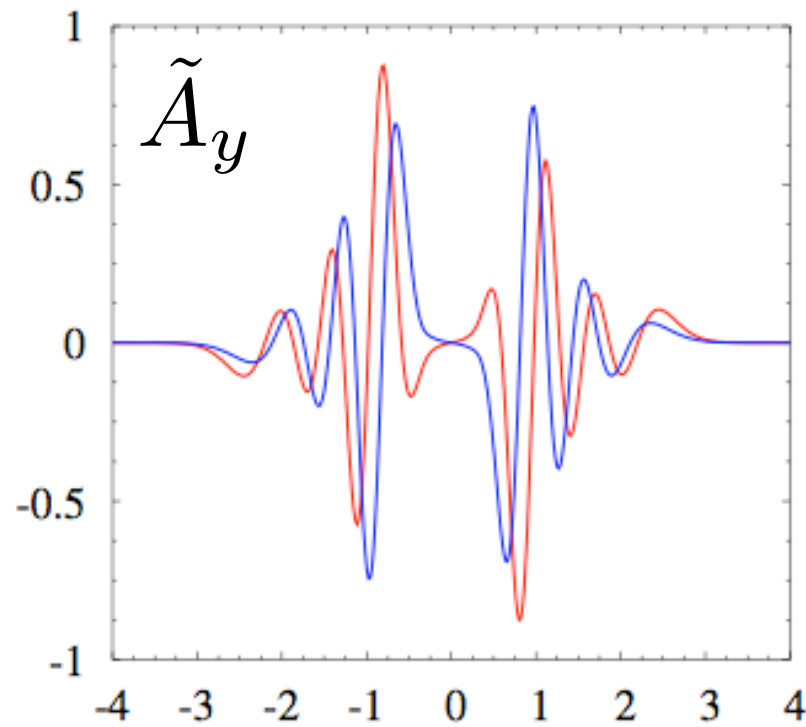
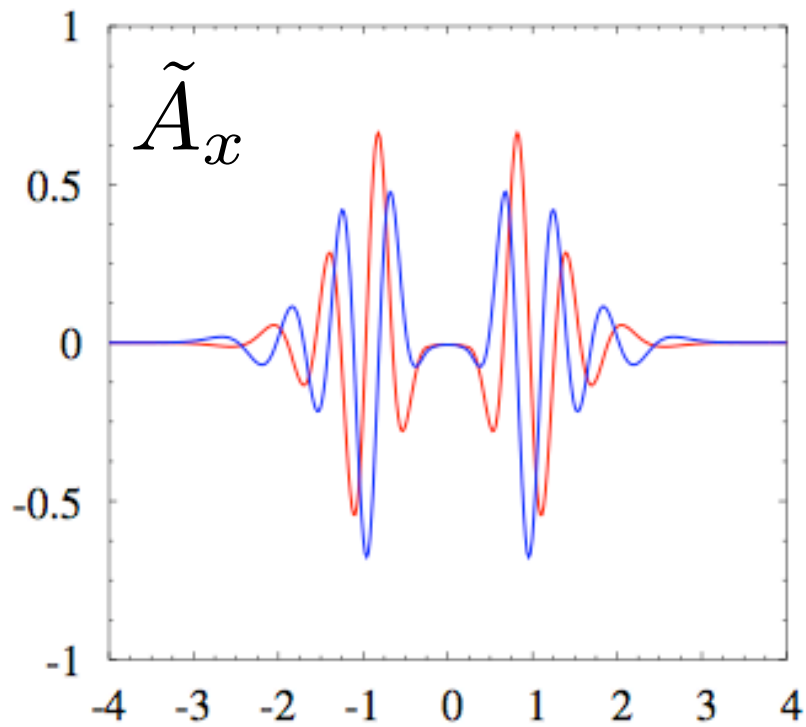


$$\nabla^2 \hat{\mathbf{A}} - \frac{1}{c^2} \frac{\partial^2 \hat{\mathbf{A}}}{\partial t^2} = -\frac{4\pi}{c} \hat{\mathbf{j}}$$

$$\nabla^2 \hat{\phi} - \frac{1}{c^2} \frac{\partial^2 \hat{\phi}}{\partial t^2} = -4\pi \hat{\rho}$$

# Short Wavelength LHDI Eigenmode

$$k_y \rho_e = 1 \Rightarrow k_y L = 11.3$$



$x/L$

$x/L$

**Eigenfunction**

$$\hat{\mathbf{A}} = \tilde{\mathbf{A}}(x) \exp[-i\omega t + ik_y y + ik_z z]$$

$$\hat{\phi} = \tilde{\phi}(x) \exp[-i\omega t + ik_y y + ik_z z]$$

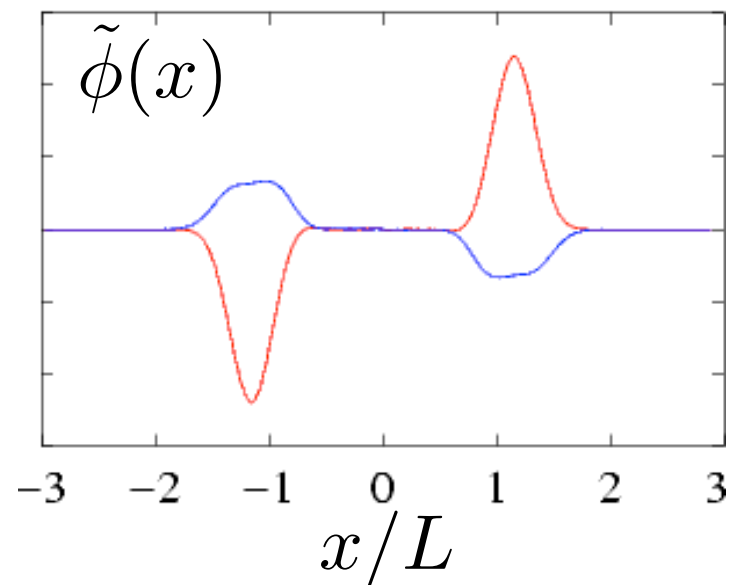
**Eigenvalue**

$$\frac{\omega_r}{\Omega_{lh}} = 0.89 \quad \frac{\gamma}{\Omega_{lh}} = 0.27$$

$$\Omega_{lh} \approx \sqrt{\Omega_{ce} \Omega_{ci}}$$

# Electrostatic Fluctuations

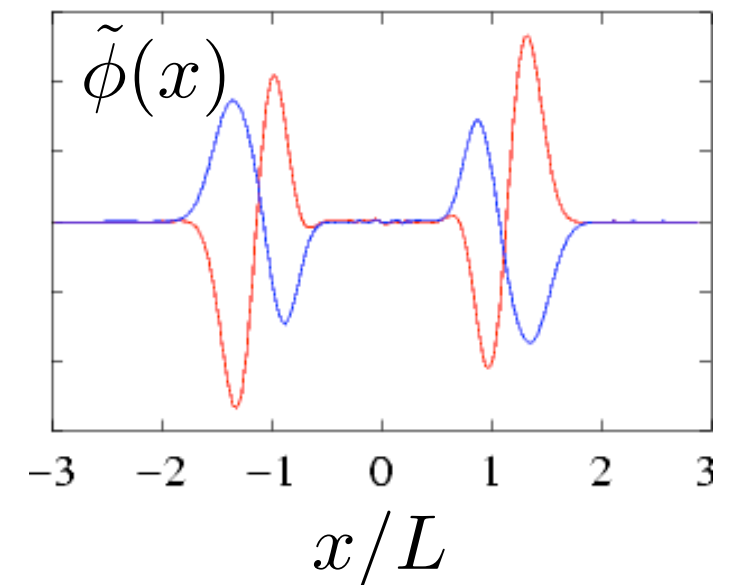
$$\omega_r / \Omega_{lh} = 0.57 \quad \gamma / \Omega_{ci} = 2.26$$



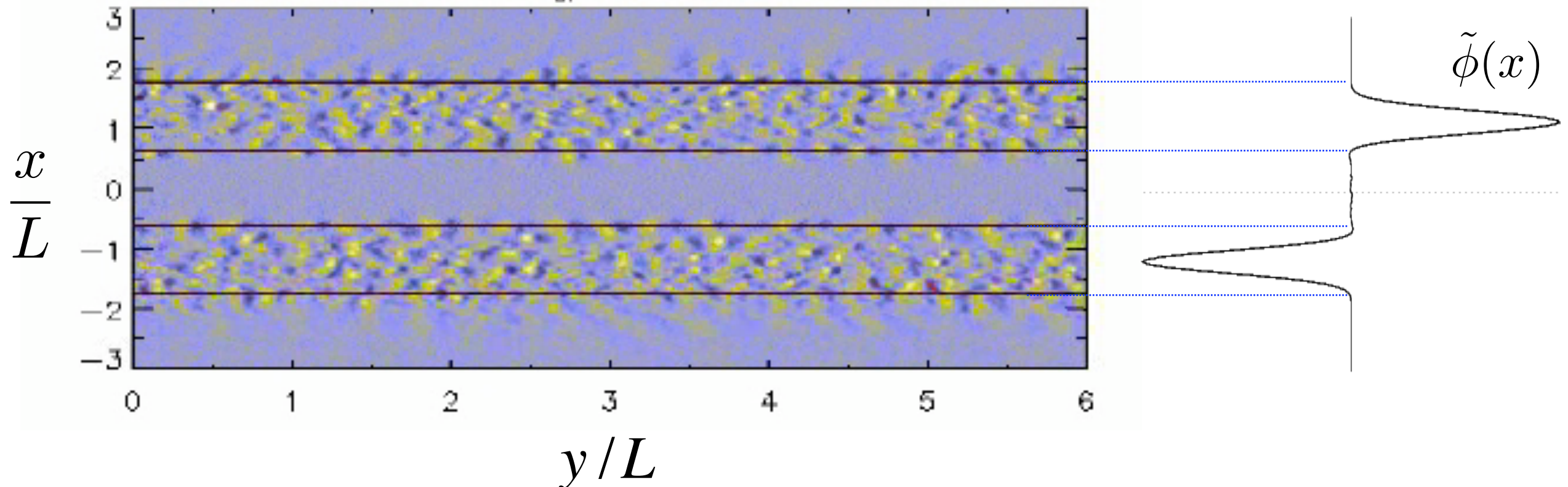
**Two fastest  
Growing  
modes**

$$k_y \rho_e \approx 0.75$$

$$\omega_r / \Omega_{lh} = 0.54 \quad \gamma / \Omega_{ci} = 1.93$$



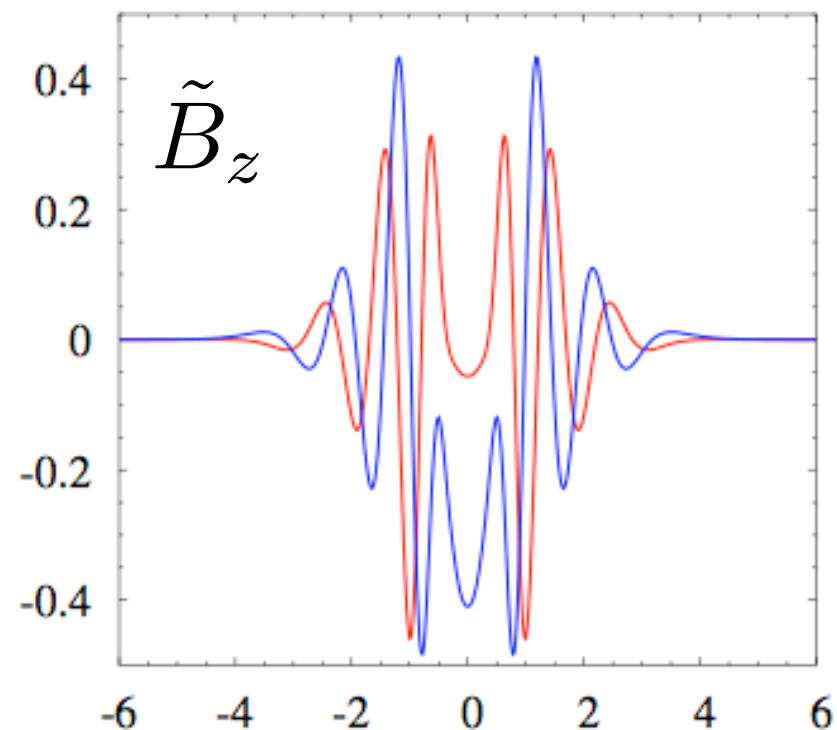
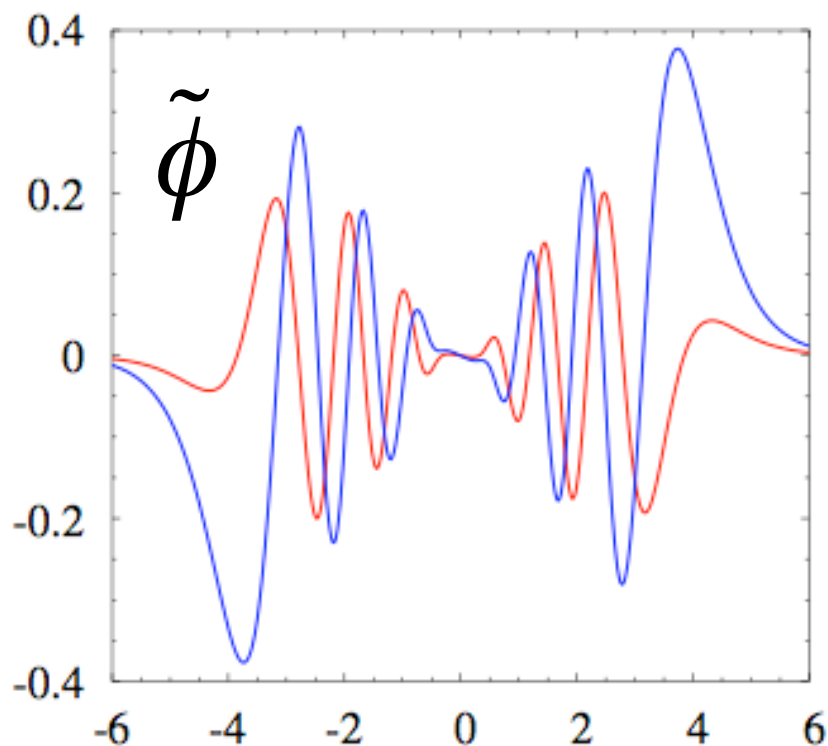
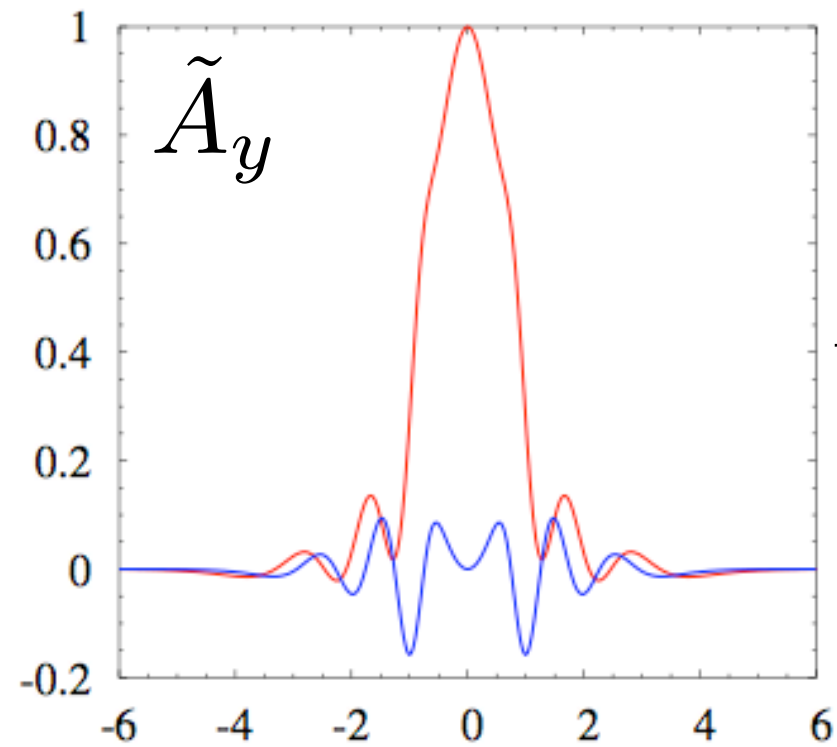
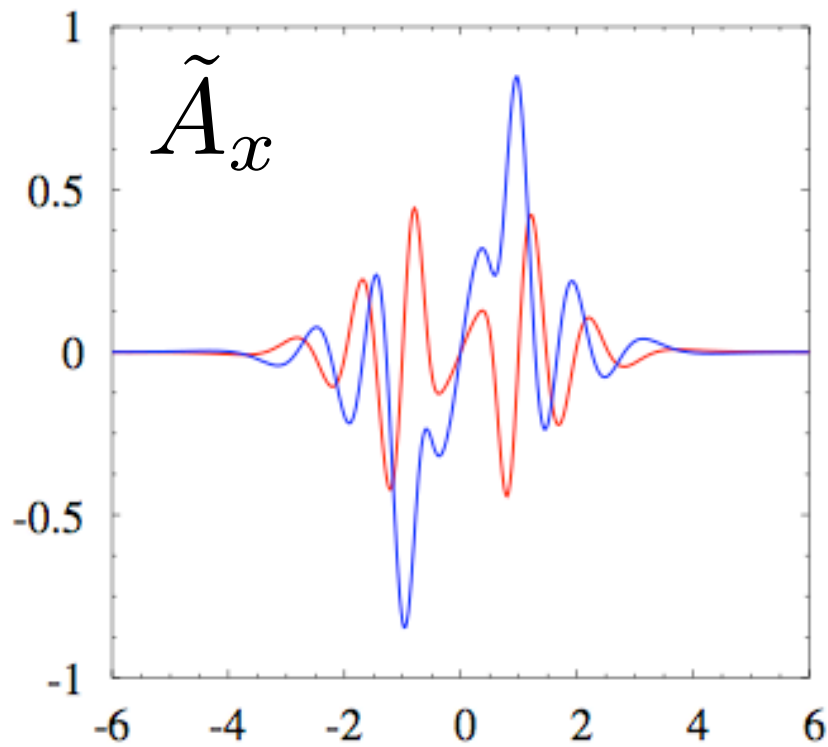
$$t \Omega_{ci} = 3.50$$



**Fluctuations are confined to the edge of the sheet**

# Longer Wavelength LHDI Eigenmode

$$k_y L = 2 \quad \Rightarrow \quad k_y \sqrt{\rho_i \rho_e} \approx 0.84$$



$x/L$

$x/L$

**Eigenfunction**

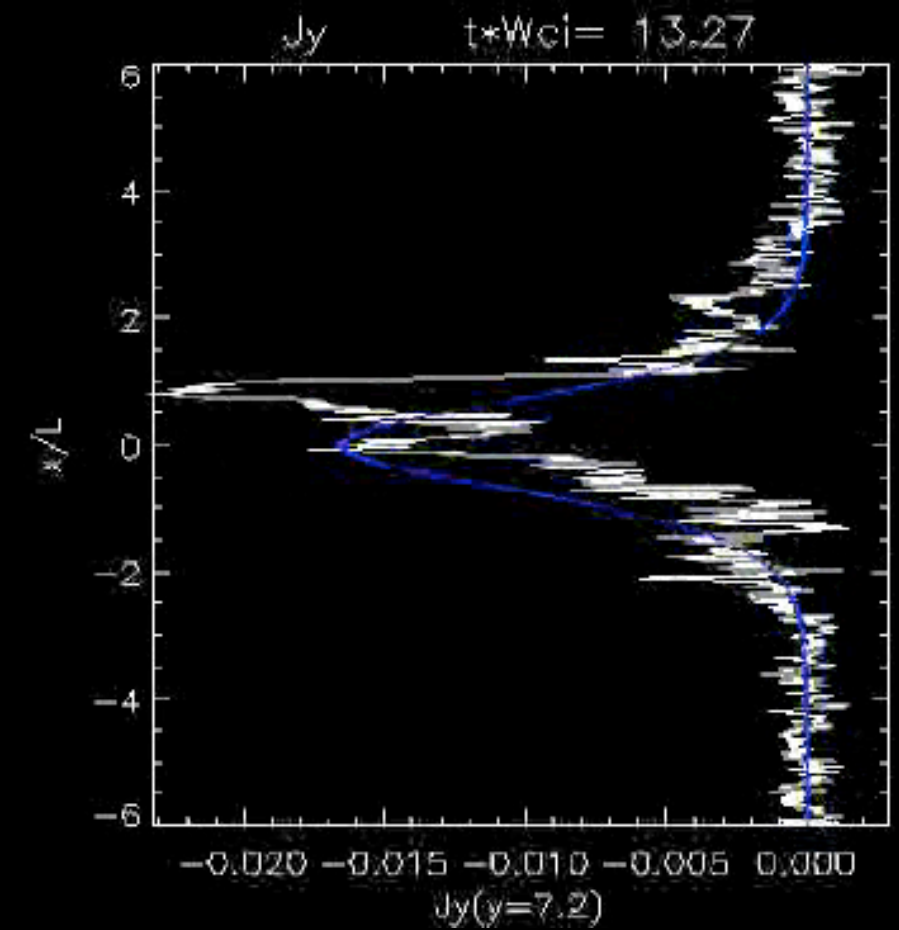
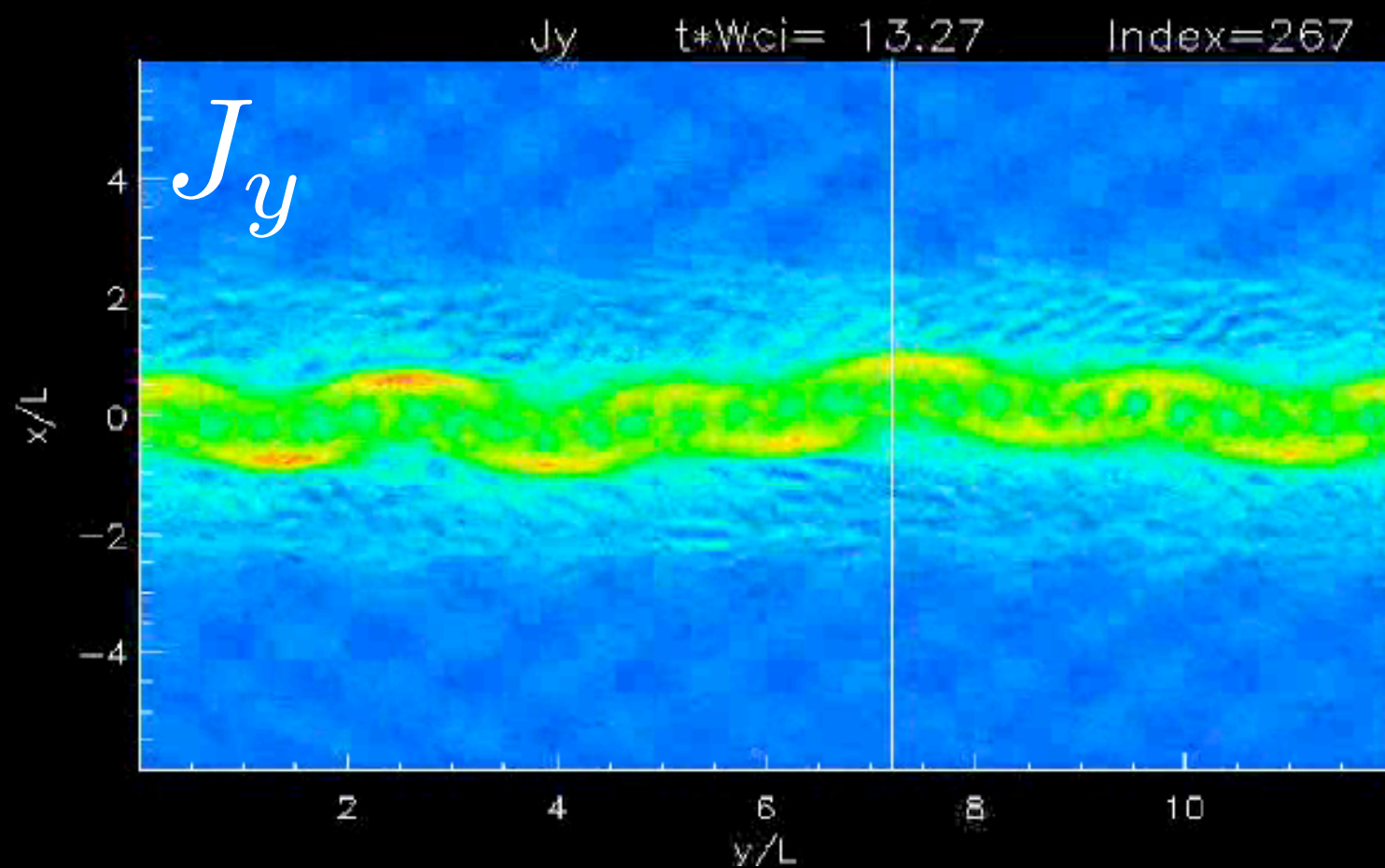
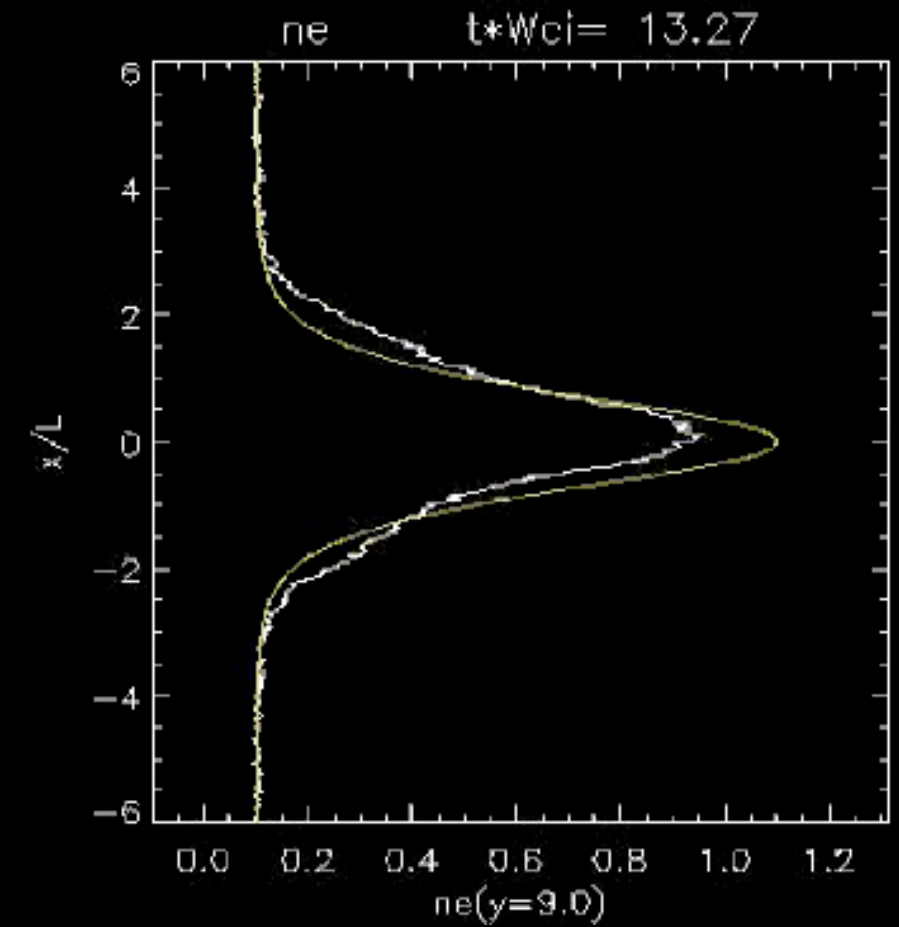
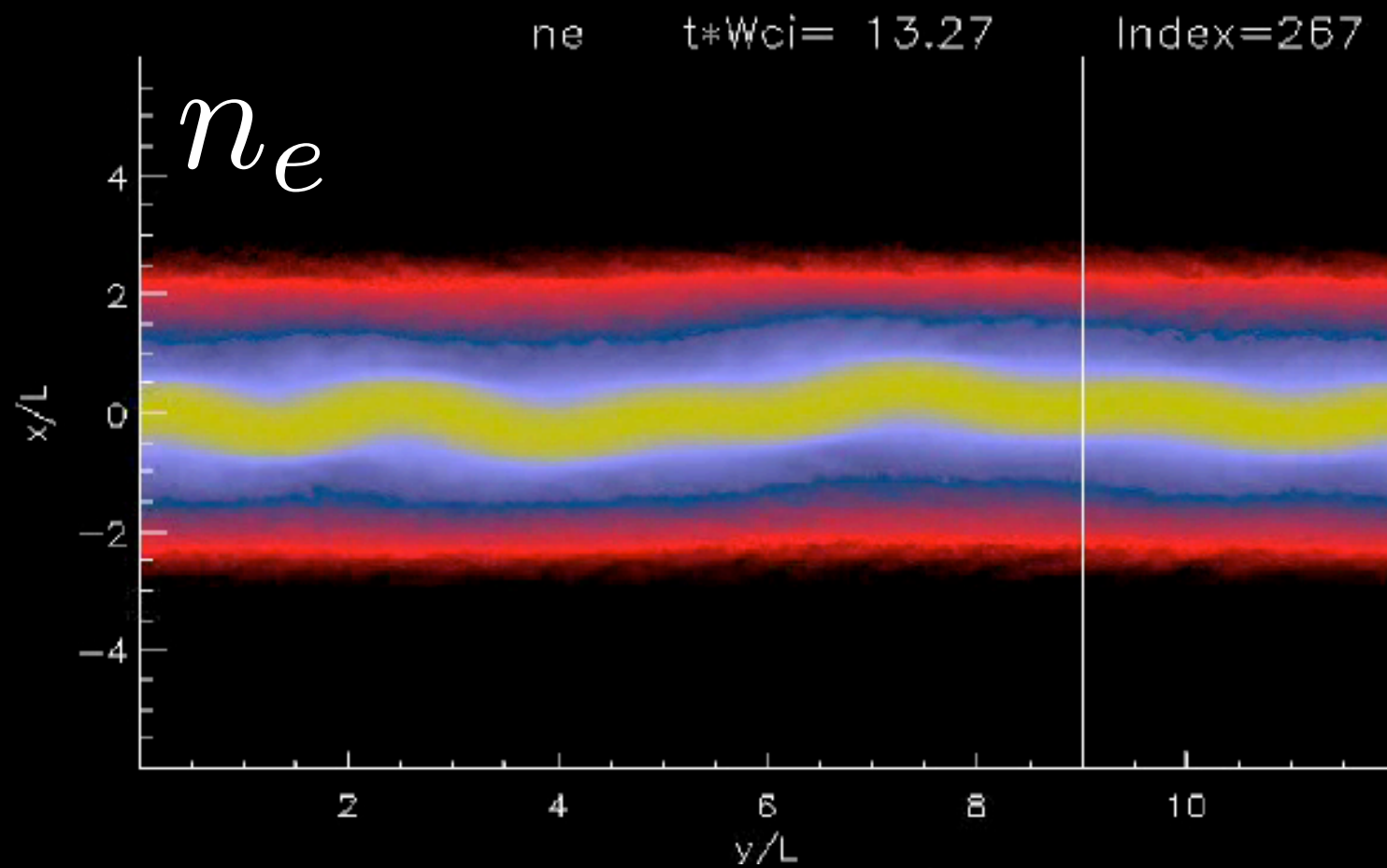
$$\hat{\mathbf{A}} = \tilde{\mathbf{A}}(x) \exp[-i\omega t + ik_y y + ik_z z]$$

$$\hat{\phi} = \tilde{\phi}(x) \exp[-i\omega t + ik_y y + ik_z z]$$

**Eigenvalue**

$$\frac{\omega_r}{\Omega_{ci}} = 6.2 \quad \frac{\gamma}{\Omega_{ci}} = 0.84$$

# Example simulation for $m_i/m_e = 1836$



# Weak Guide Field Example

$$\frac{\rho_i}{L} = 5.77, \quad \frac{m_i}{m_e} = 1836, \quad \frac{\omega_{pe}}{\Omega_{ce}} = 4, \quad \frac{T_i}{T_e} = 10, \quad B_{yo}/B_{xo} = 0.2 \quad n_o/n_b = 0.1923$$

$$k_y L = 1.7$$



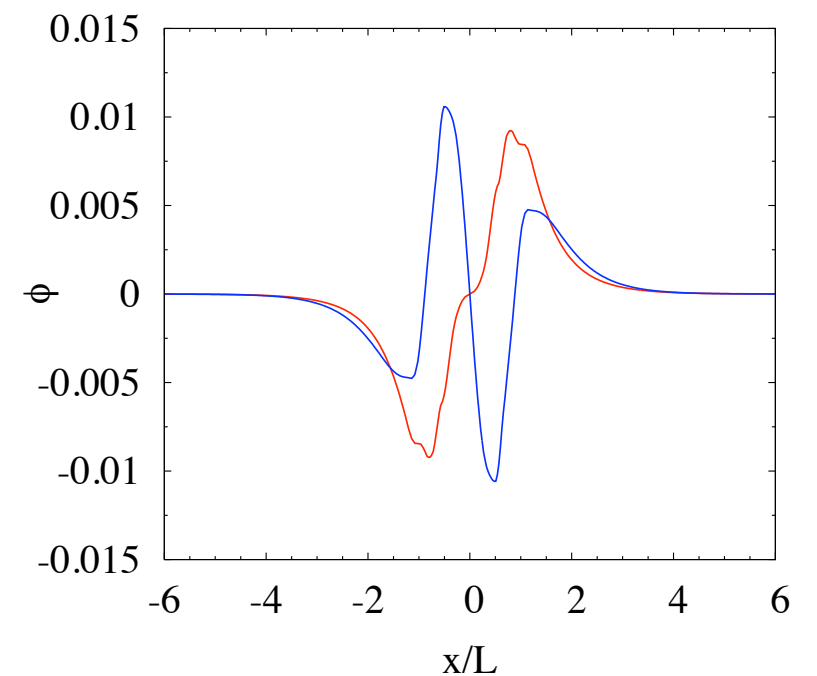
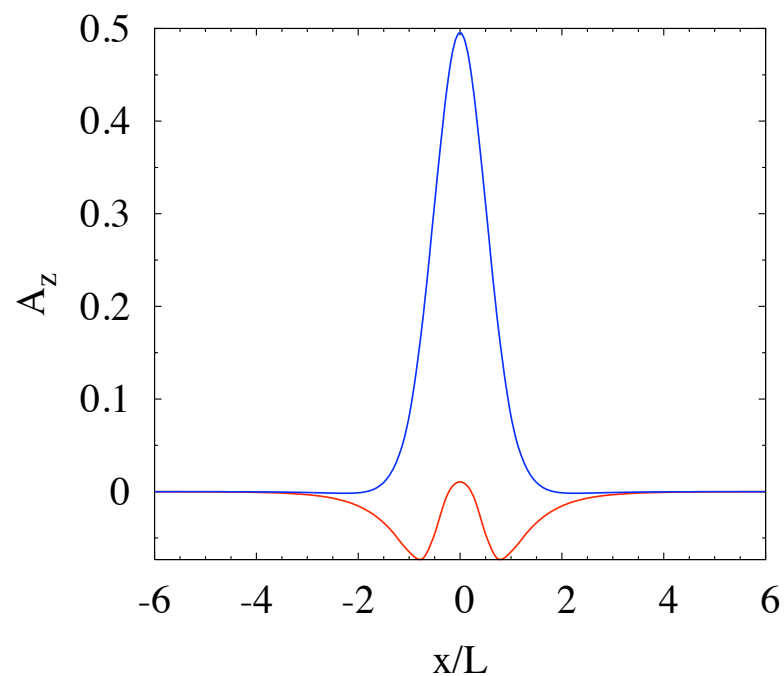
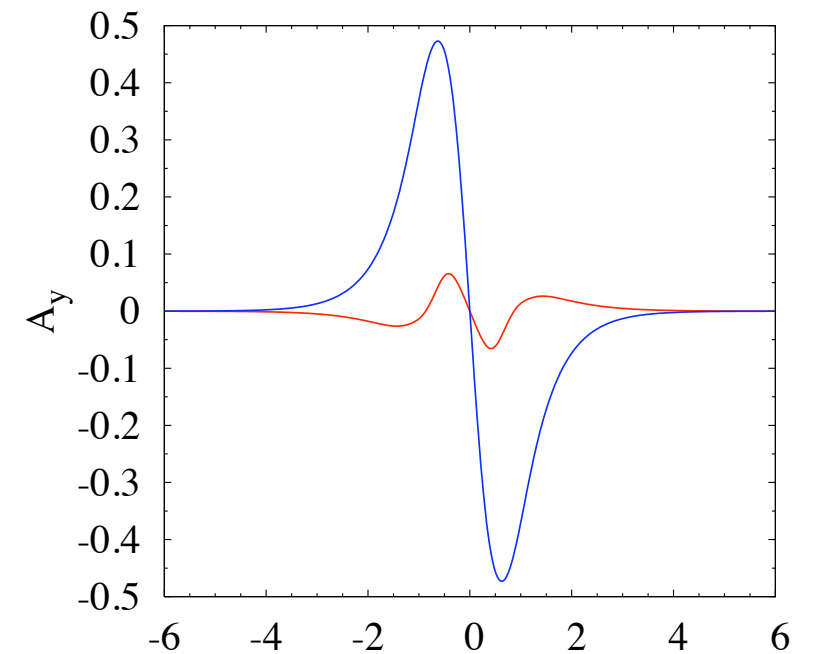
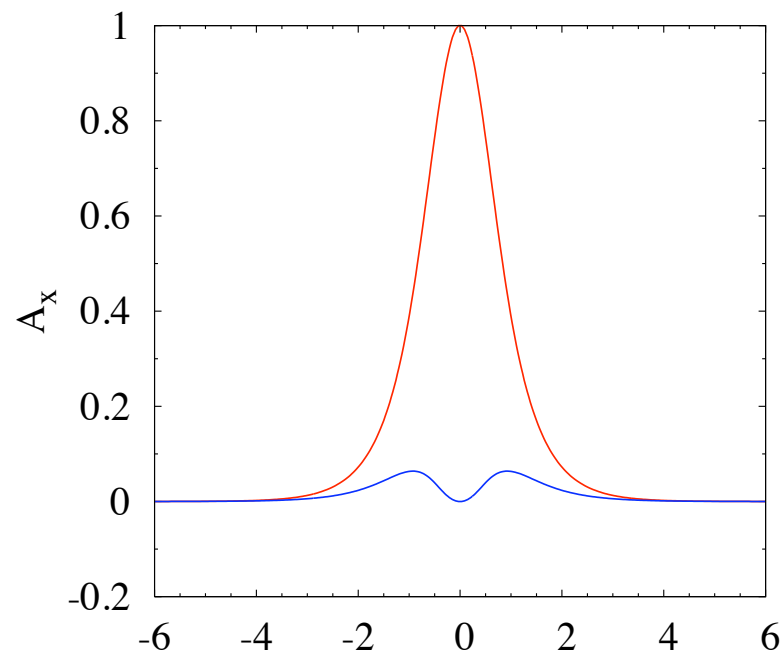
$$k_y (\rho_i \rho_e)^{1/2} \approx 0.85$$



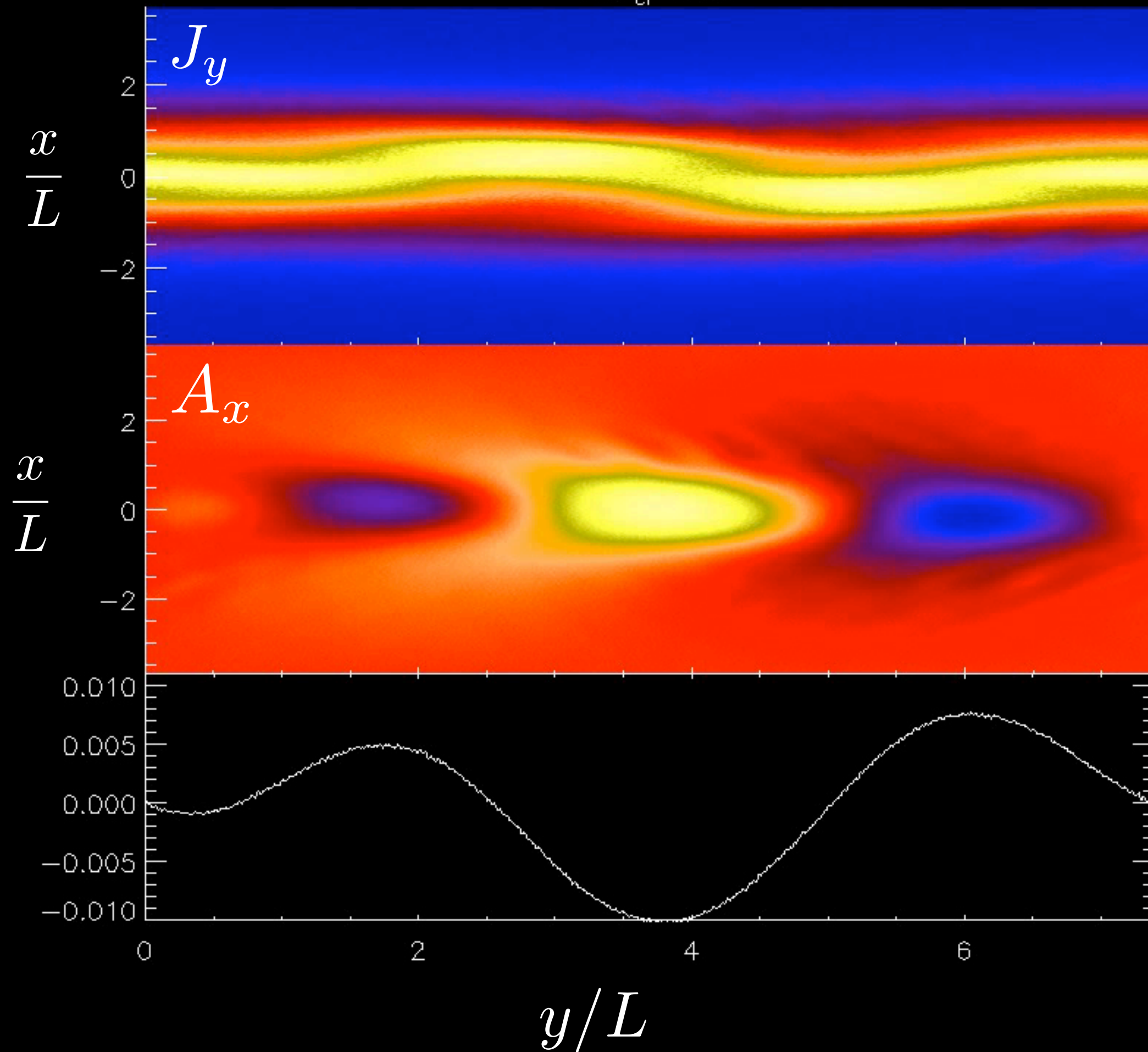
**Vlasov  
Theory**

$$\gamma / \Omega_{ci} \approx 1.87$$

$$\omega / \Omega_{ci} \approx 53.4$$



$t * \Omega_{ci} = 3.24$



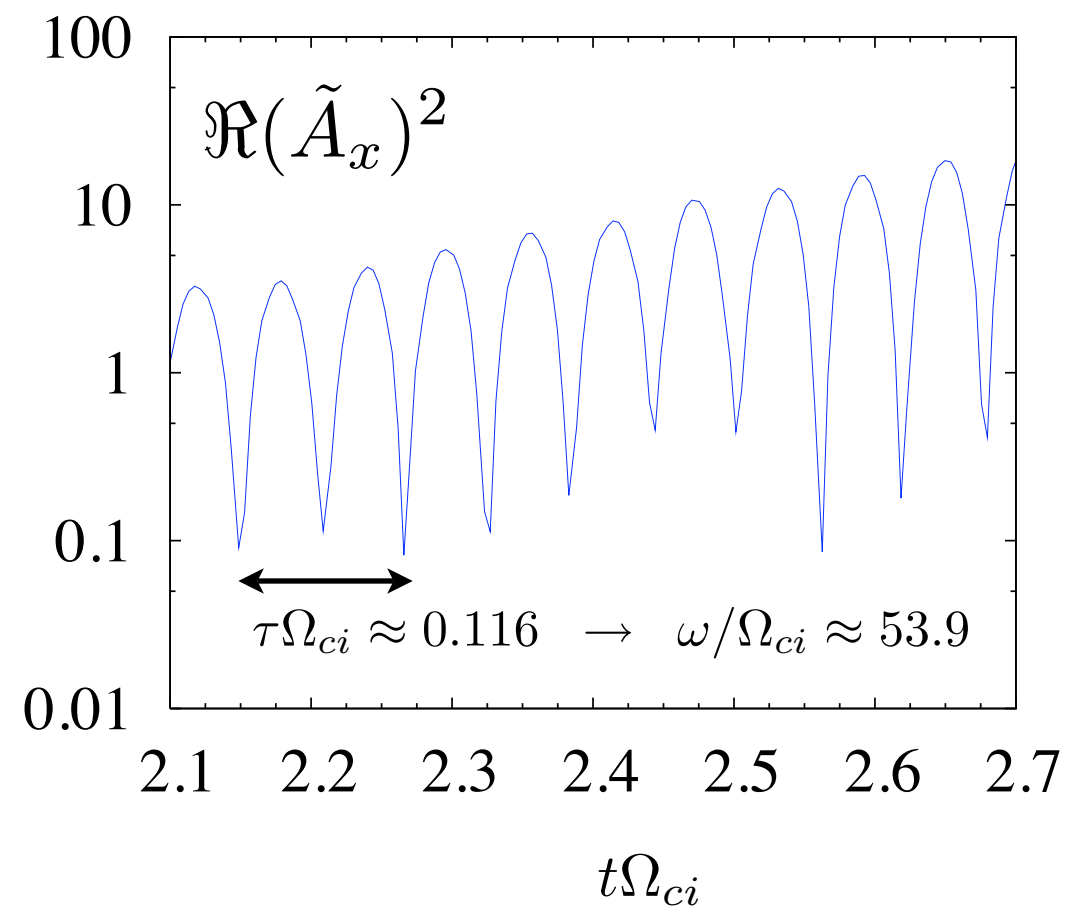
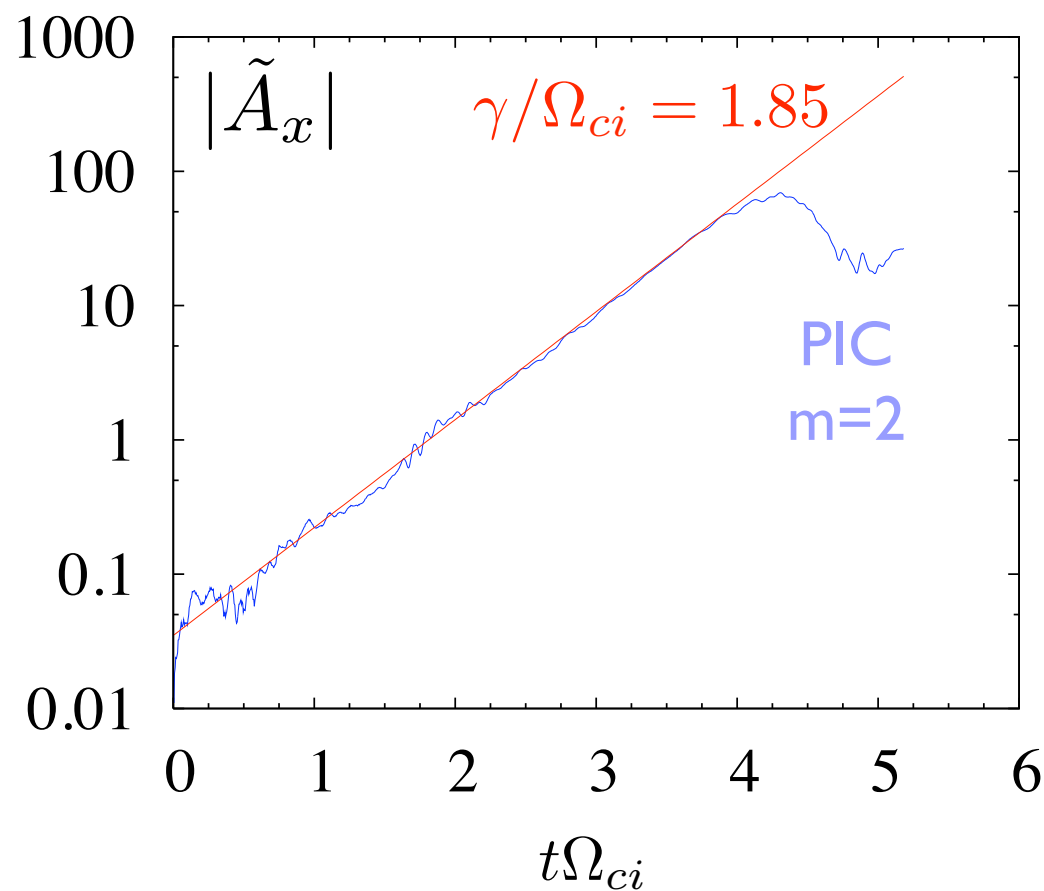
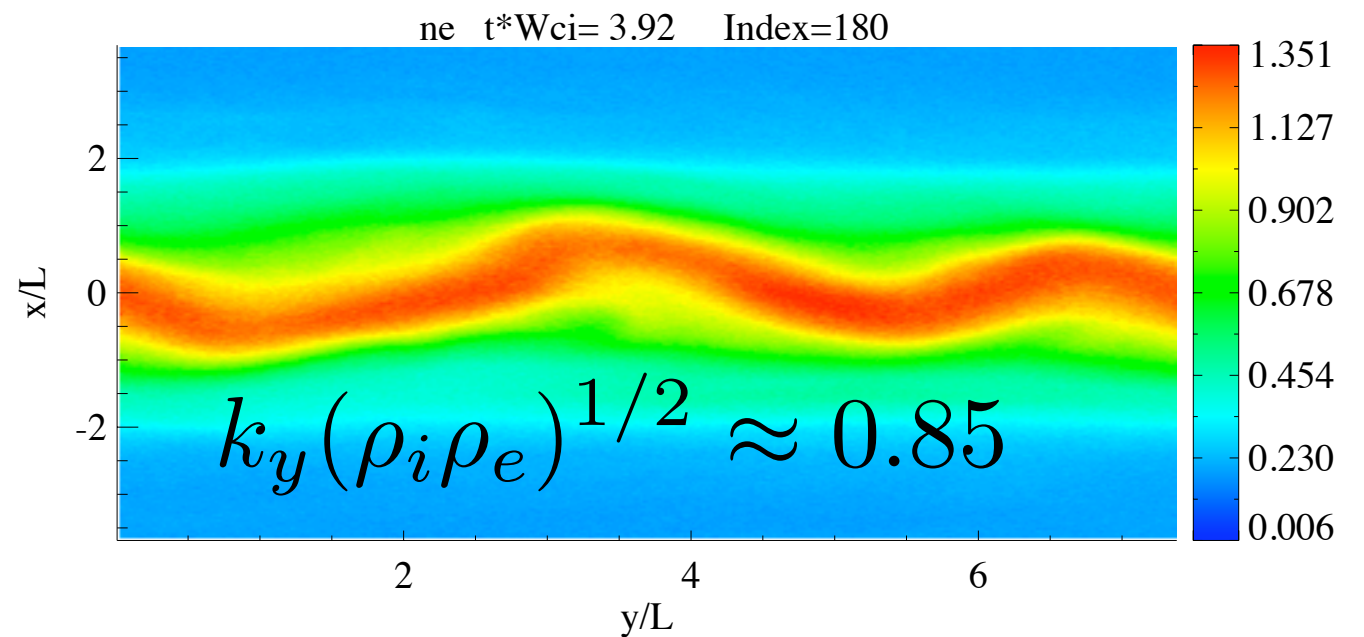
# Weak Guide Field Example

$$\frac{\rho_i}{L} = 5.77, \quad \frac{m_i}{m_e} = 1836, \quad \frac{\omega_{pe}}{\Omega_{ce}} = 4, \quad \frac{T_i}{T_e} = 10, \quad B_{yo}/B_{xo} = 0.2 \quad n_o/n_b = 0.1923$$

Vlasov  
Theory

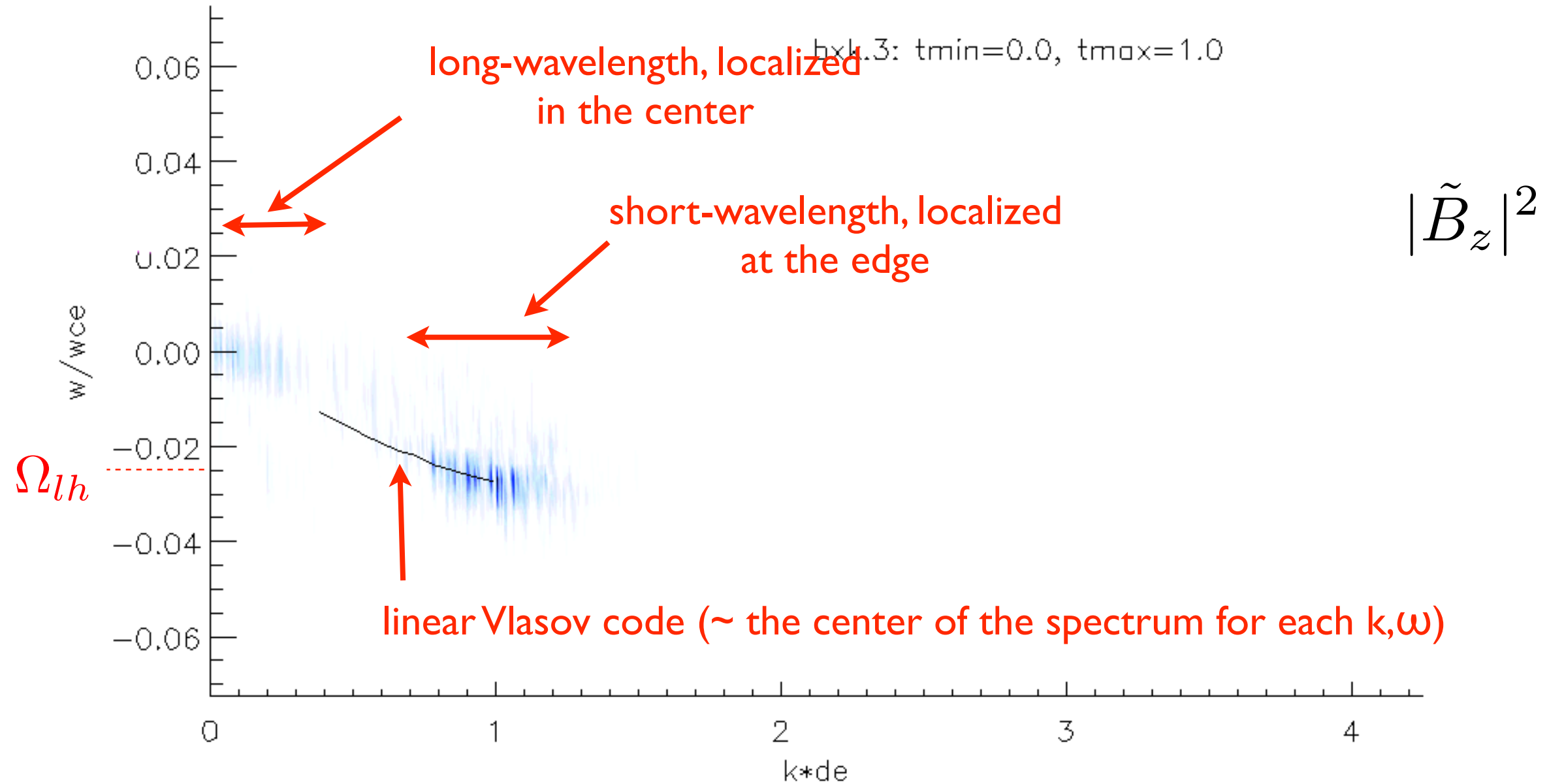
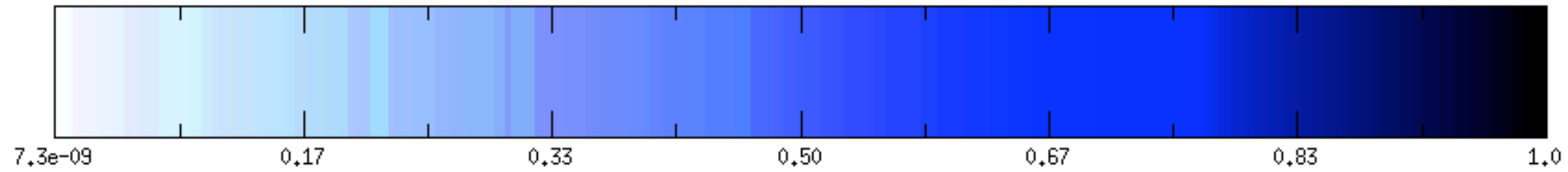
$$\gamma/\Omega_{ci} \approx 1.87$$

$$\omega/\Omega_{ci} \approx 53.4$$

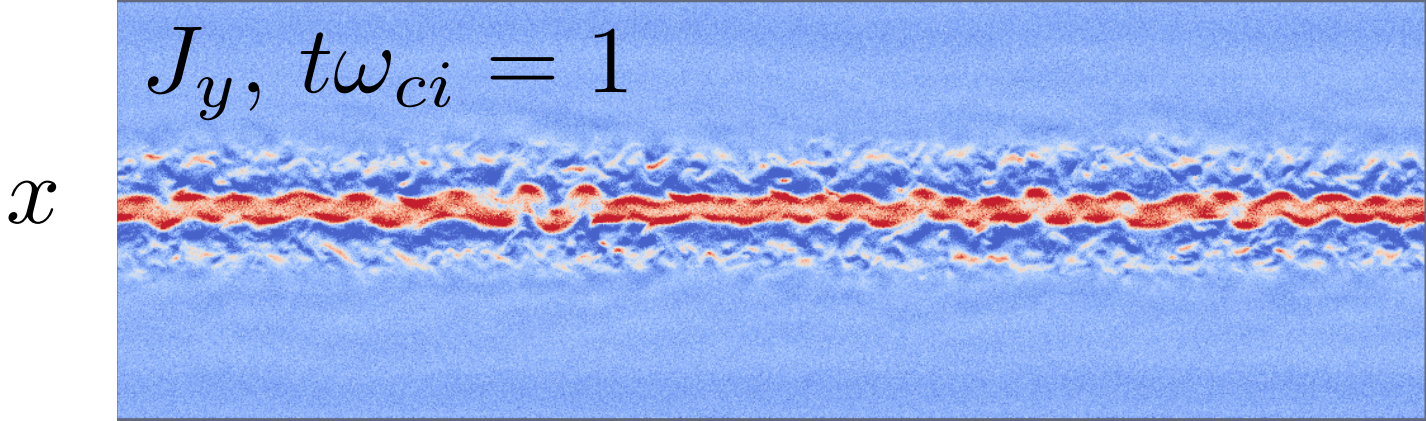


# Example frequency spectrum for 2D Harris sheet

$$m_i/m_e = 1836$$



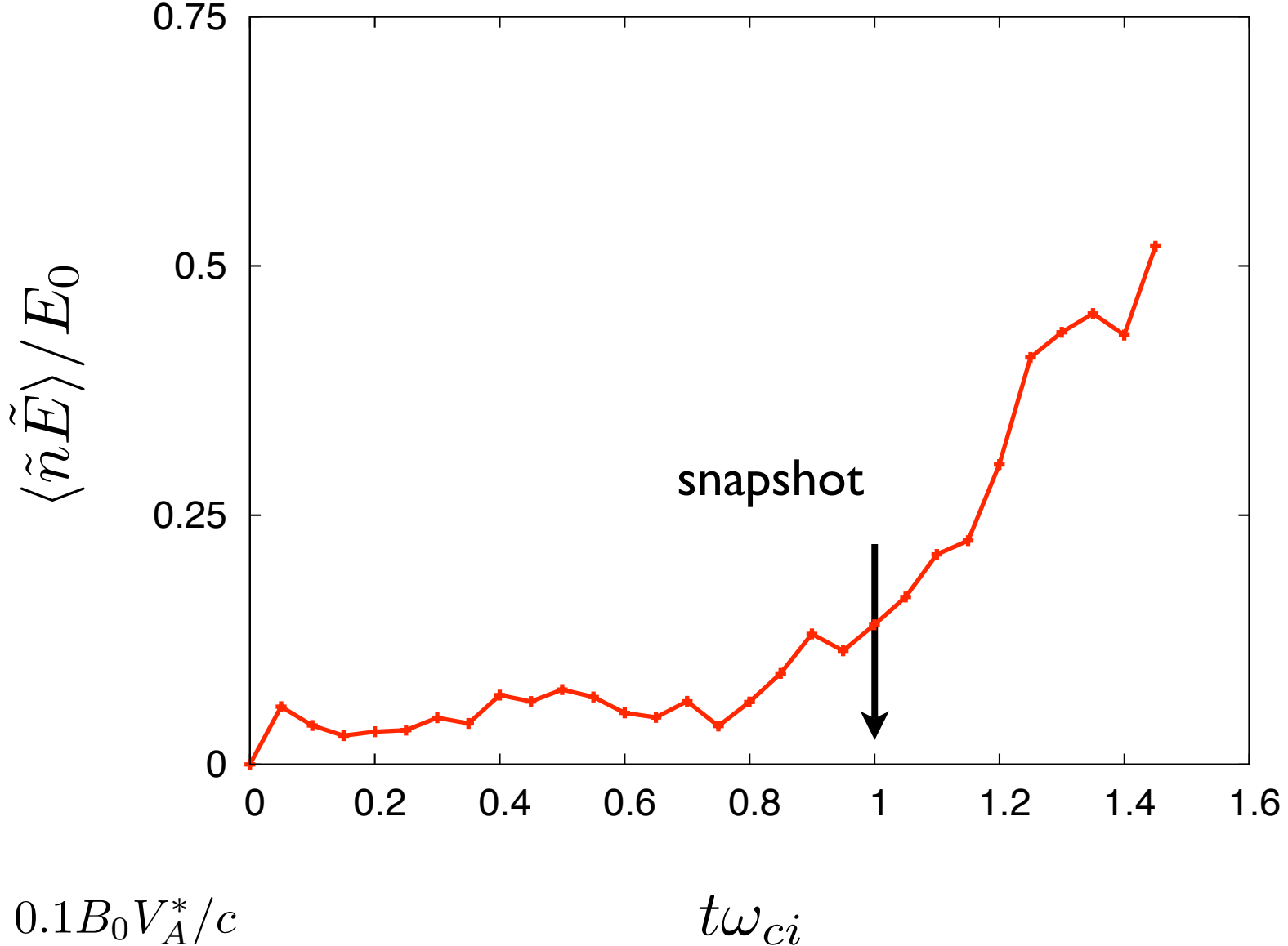
# The instability is very strong in Harris equilibrium



2D simulation, Harris current sheet with  $\delta/\rho_e=10; m_i/m_e=1836; n_B=0.3$

$y$

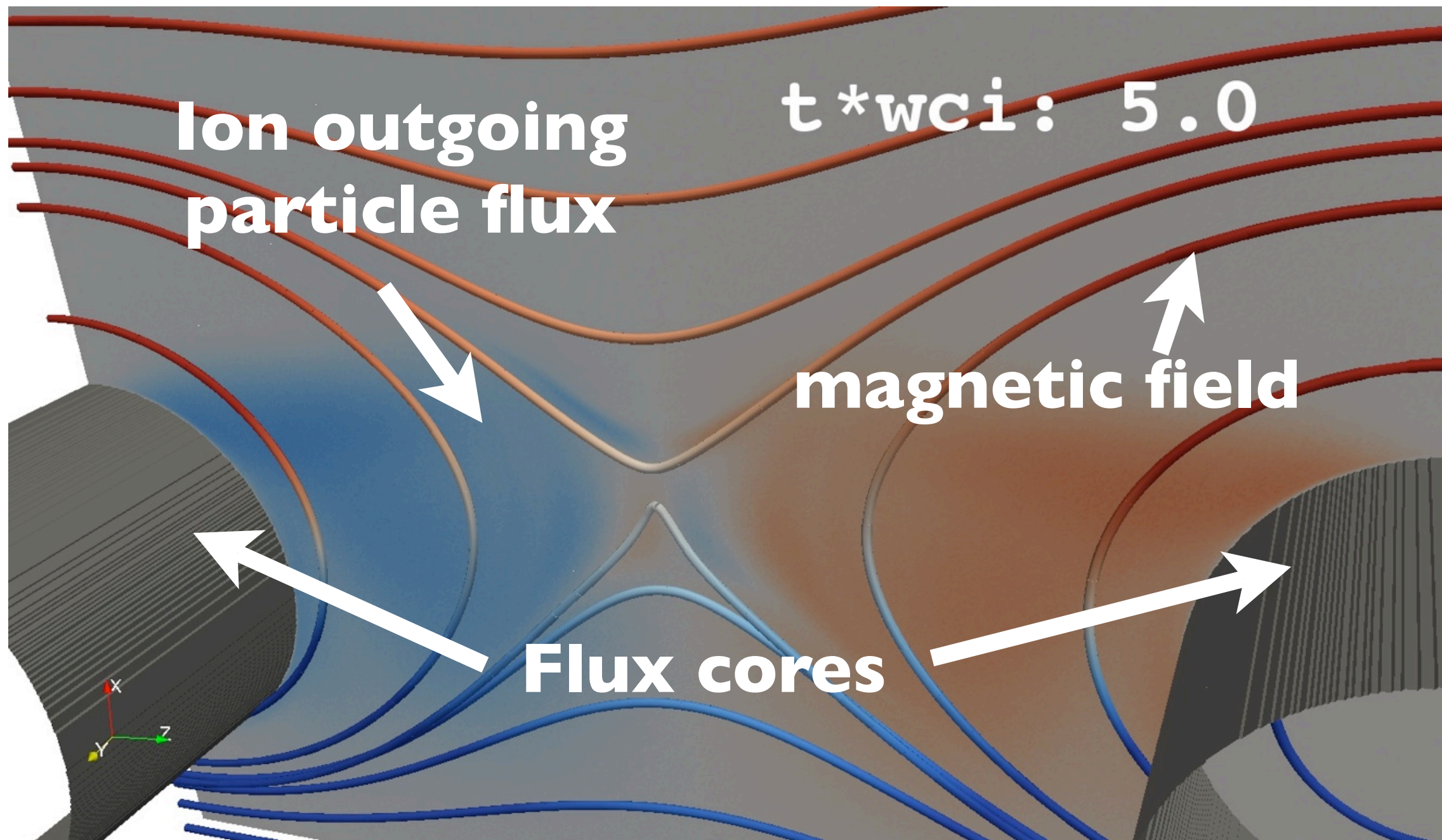
The mode induces sizable momentum exchange between electrons and ions, but only when the amplitude becomes quite large



$E_0 = 0.1B_0V_A^*/c$

# 3D Simulations

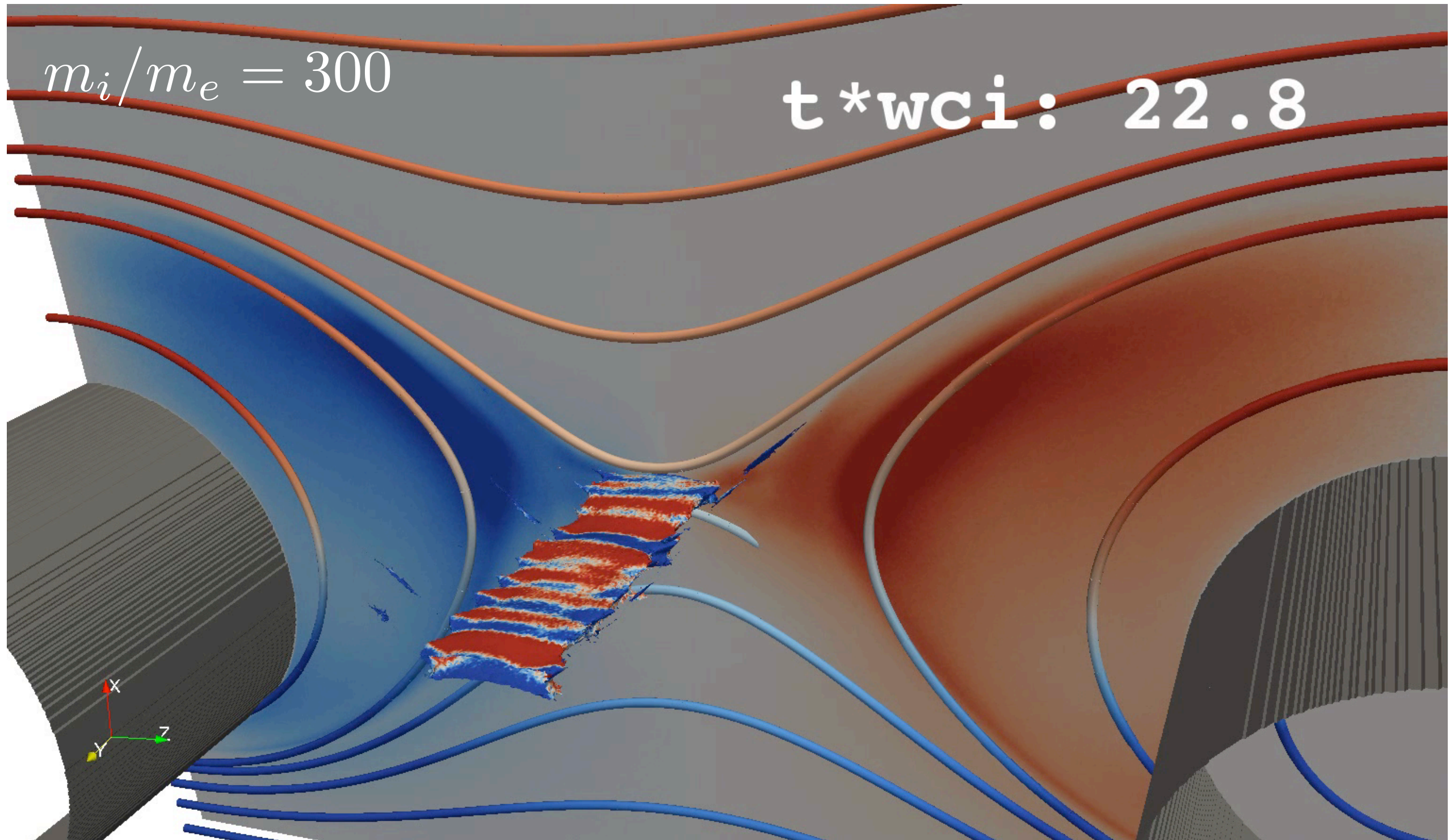
# 3D simulations shows that under conditions typical of MRX, the layers are unstable against multiple instabilities



$$n_0 = 2 \cdot 10^{13} \text{cm}^{-3}, m_i/m_e = 300, (\nu_{ei}/\Omega_{ce}) \approx 0.01, (9 \times 3 \times 11.5) d_i^0$$

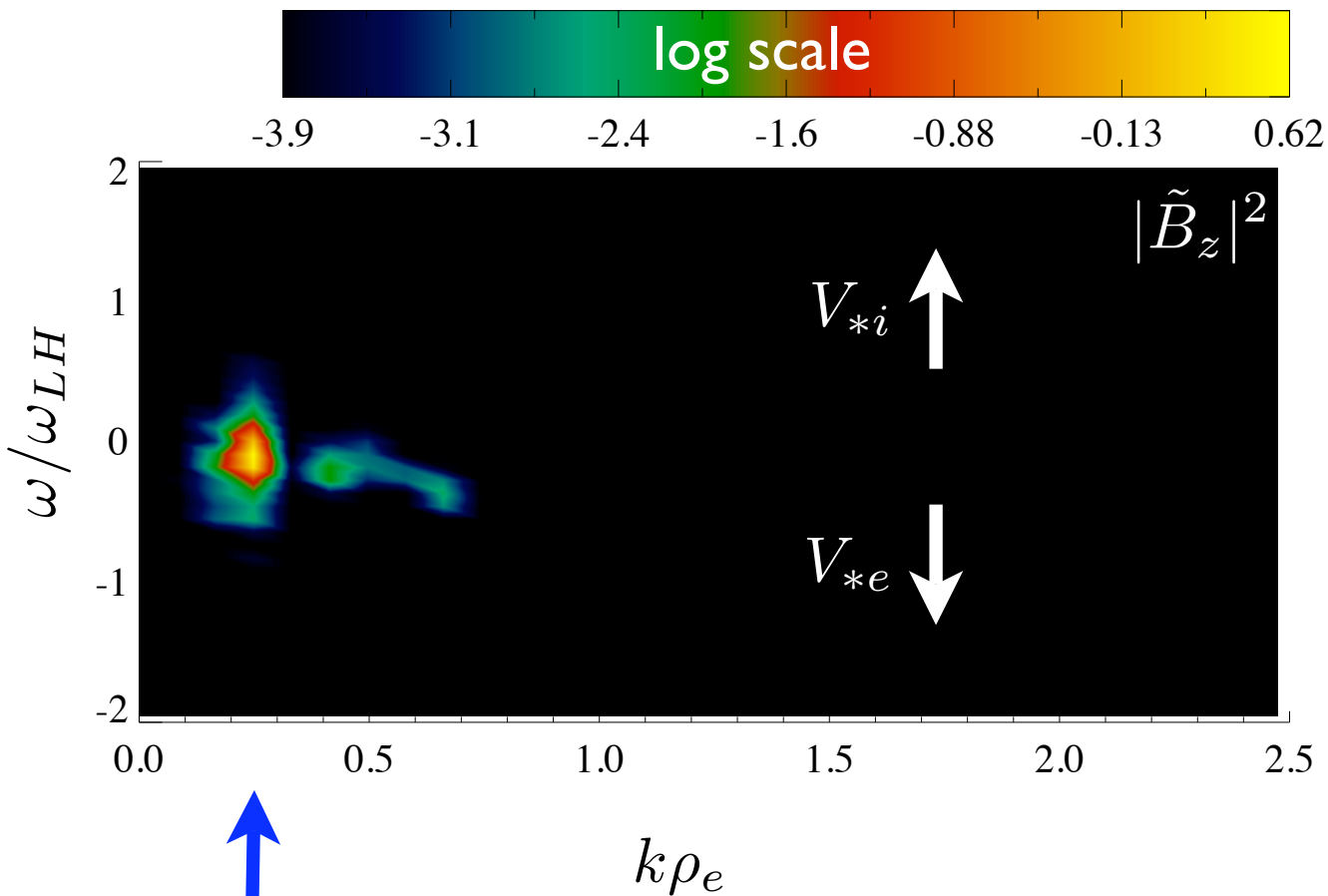
0.72 billion cells, 158 billion particles, 2880 MPI ranks on Roadrunner

# 3D simulations shows that under conditions typical of MRX, the layers are unstable against multiple instabilities

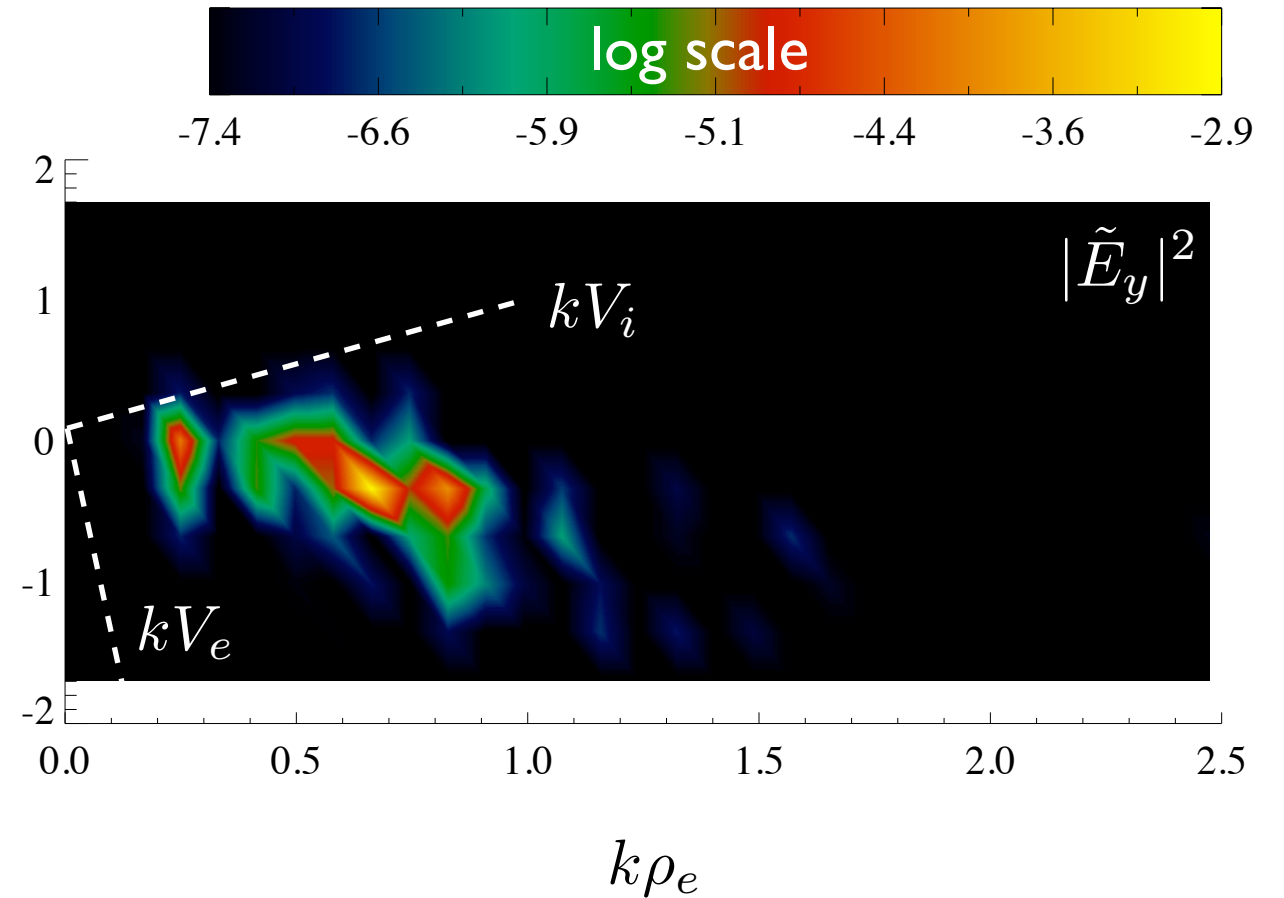


# The range of unstable $k, \omega$ is close to MRX observations

magnetic fluctuations (center)

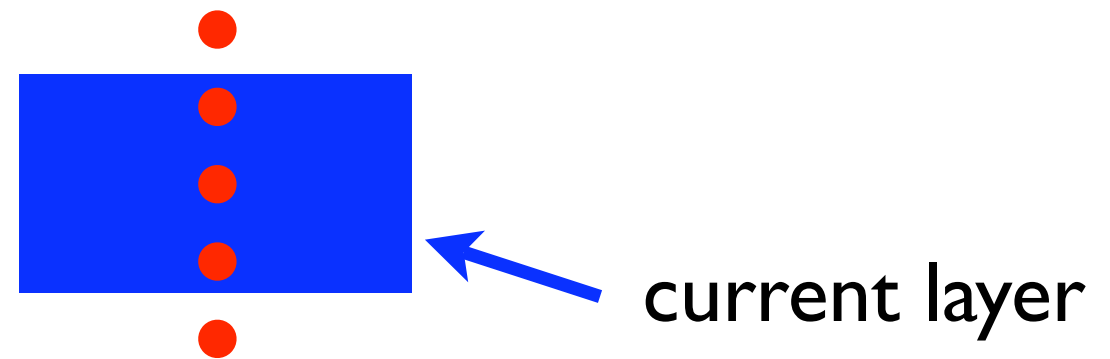


electric field fluctuations (edge)

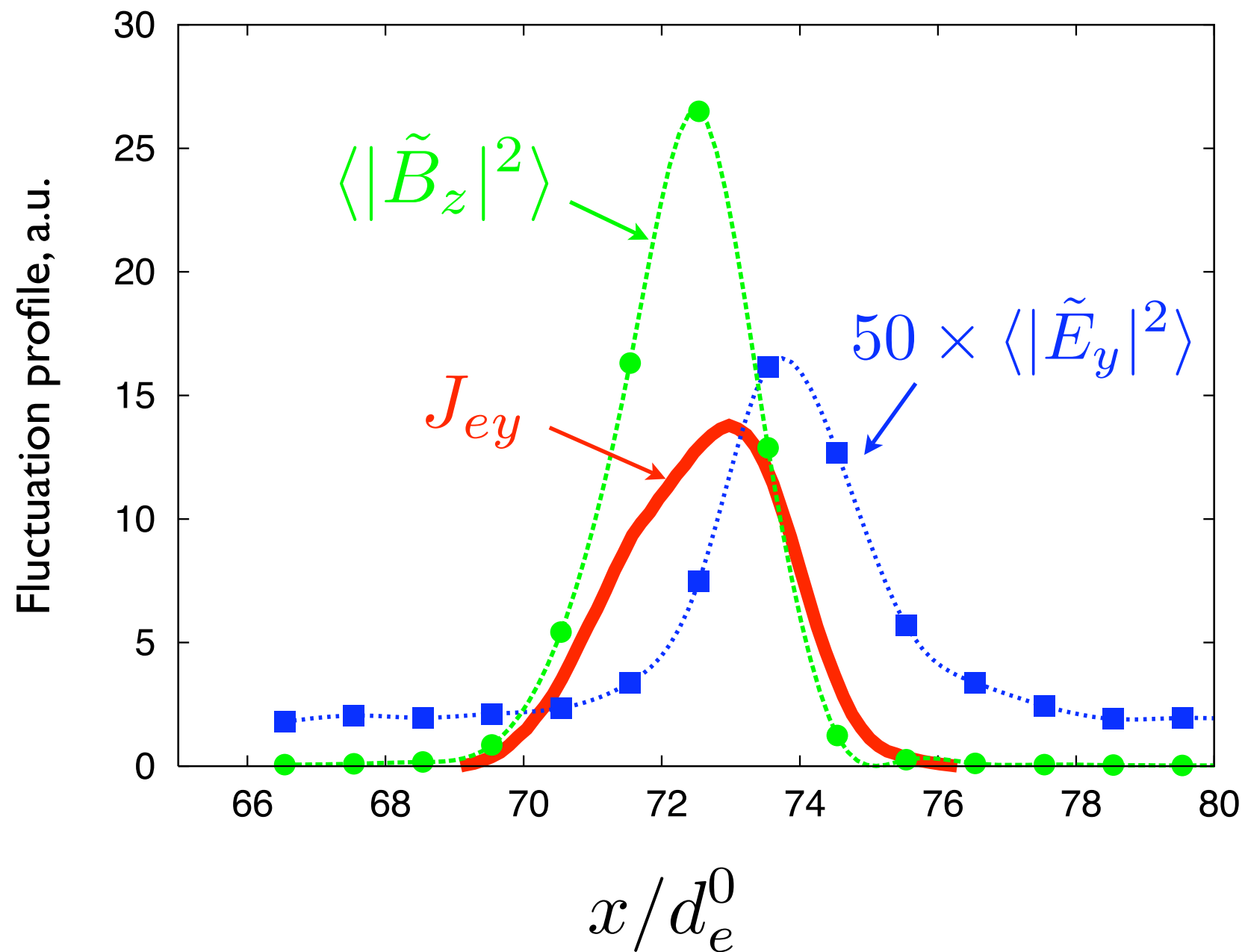


$k(\rho_e \rho_i)^{1/2} \sim 1$

location of the  
“probes”



# Mode localization is similar to MRX observations



Similar to MRX observations, electric field fluctuations are localized at the edge of the layer, while magnetic fluctuations peak at the center

**Linking MRX observations and instabilities in collisionless (e.g. magnetospheric) plasmas**

# Asymmetric configuration (relevant to the magnetopause)

The initial state is not a Vlasov equilibrium,  
but is in a pressure balance.

The asymmetry is preserved as  
reconnection proceeds

$$n(T_e + T_i) + \frac{B_z^2}{8\pi} = \text{Const}$$

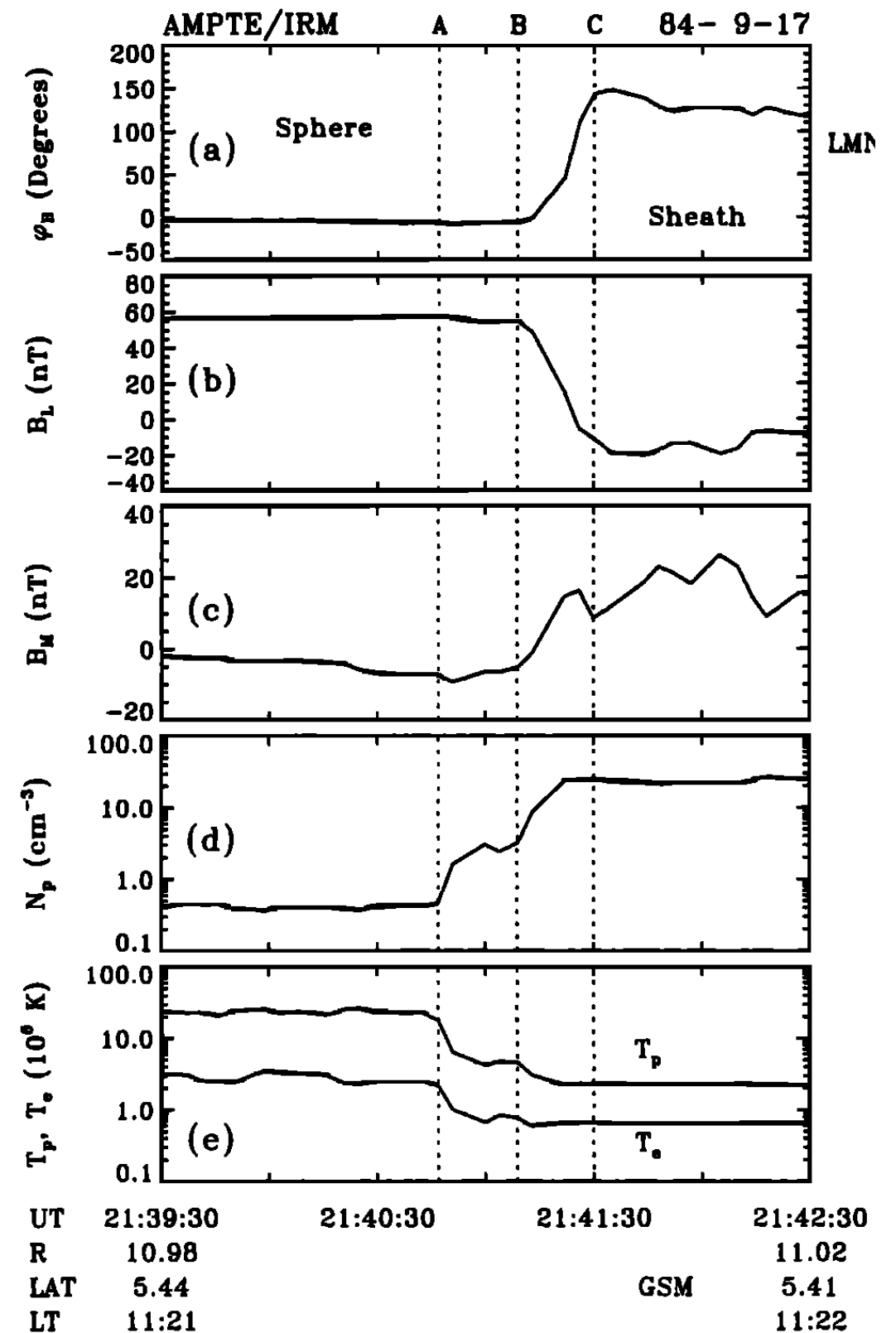
$$B_z = B_s + B_H \tanh(x/\delta)$$

$$n = n_c - \delta n \tanh(x/\delta) + \frac{n_H^0}{\cosh^2(x/\delta)}$$

$$T_e, T_i = \text{const}$$

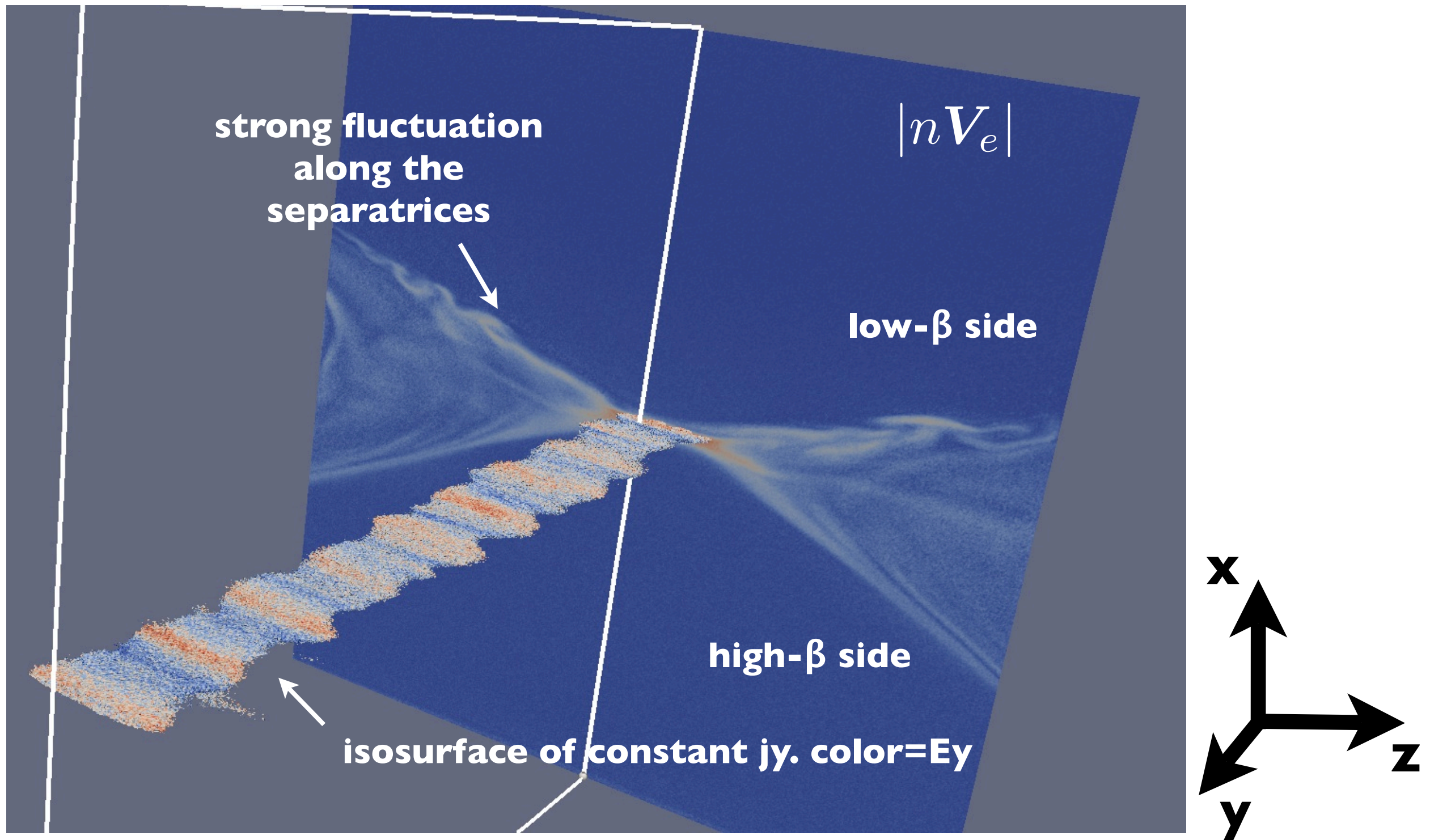
we specify the equilibrium by prescribing  
the value of plasma beta on one side of  
the sheet and the ratio of densities  
between the two sides. Examples shown  
are from simulations with:

$$\beta_{|x \rightarrow -\infty} = 1 \quad n_{-\infty}/n_{+\infty} = 5 \quad T_e/T_i = 1$$



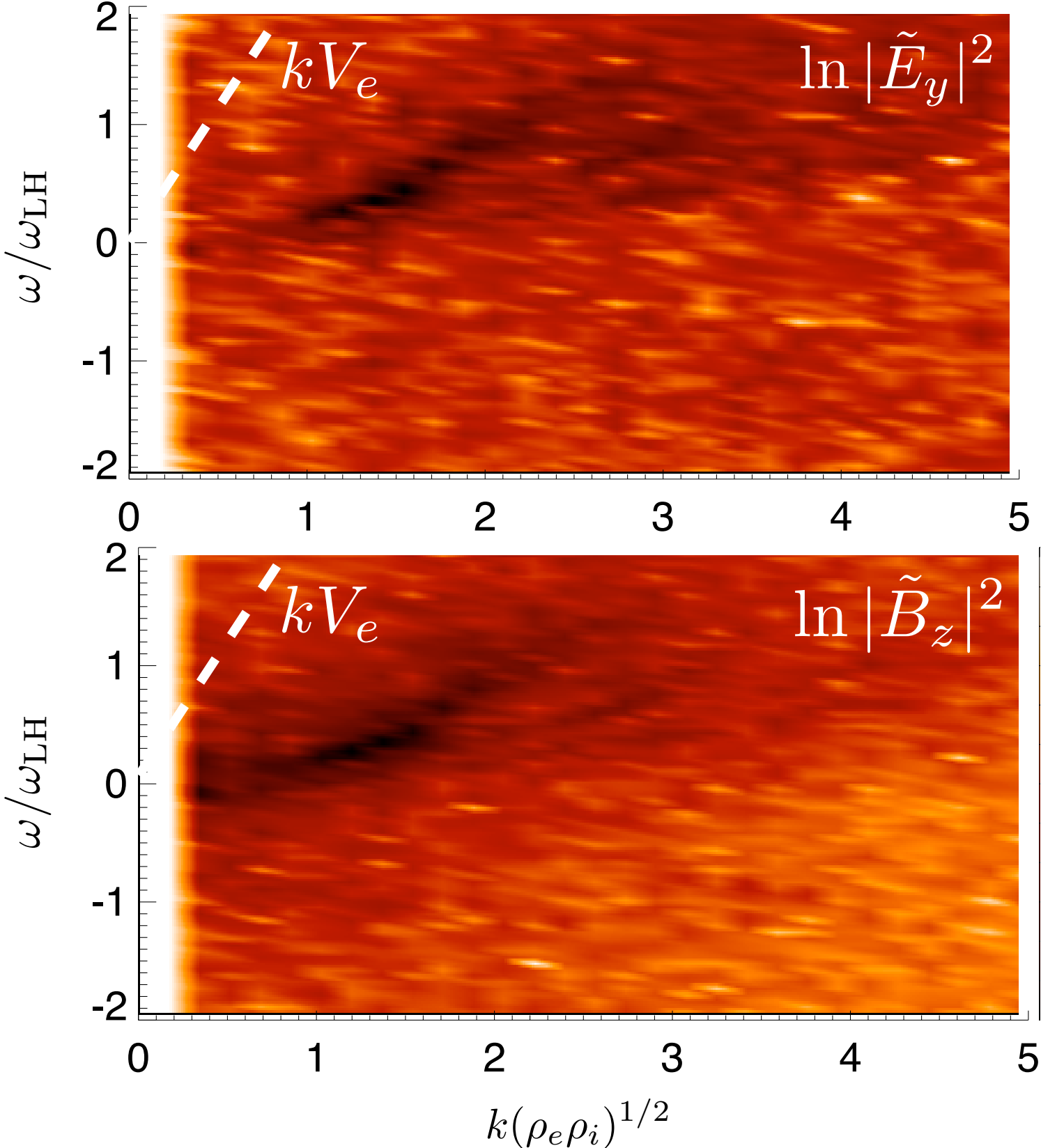
MP current sheet structure  
(Phan and Paschmann, JGR, 1996)

# At higher mass ratio, instability saturates at modest amplitude



Asymmetric configuration,  $(10 \times 10 \times 10)d_i$  based on the upstream high  $n$   
Open boundary driven simulation,  $m_i/m_e=400$ ,  $810^3$  cells,  $3.2 \times 10^{11}$  particles at  $t=0$

# Spectrum near center is similar



Open-boundary, asymmetric configuration,  $m_i/m_e=400$

# The mode produces finite modifications to the Ohm's law

Consider y-averaged electron momentum balance

$$\left\langle ne \left( \mathbf{E} + \frac{1}{c} \mathbf{v} \times \mathbf{B} \right) \right\rangle = -\nabla \cdot \langle P_e \rangle - m_e \left\langle n \frac{d\mathbf{V}_e}{dt} \right\rangle$$

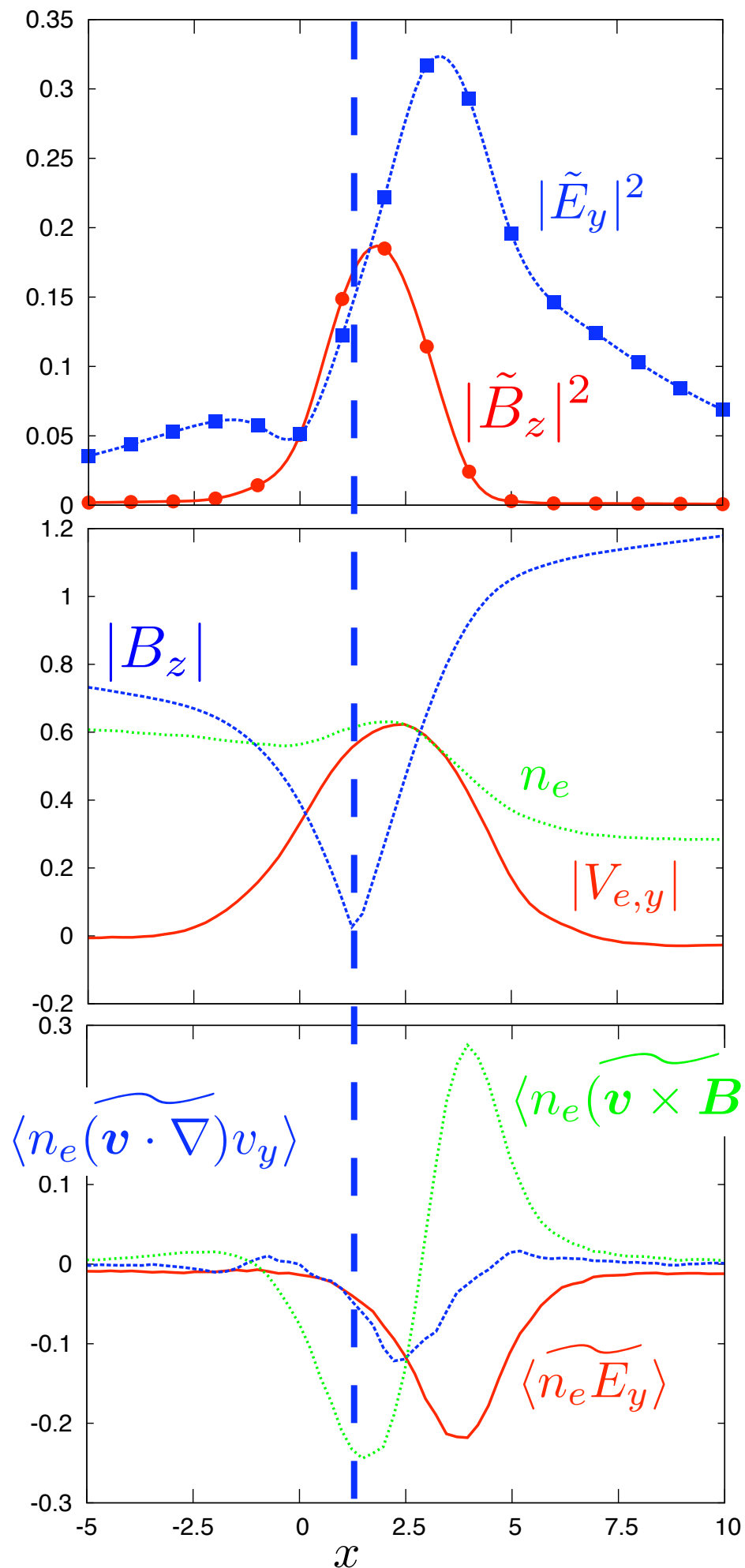
Split non-linear terms

$$\langle AB \rangle = \langle A \rangle \langle B \rangle + \widetilde{\langle AB \rangle} \quad \langle ABC \rangle = \langle A \rangle \langle B \rangle \langle C \rangle + \widetilde{\langle ABC \rangle}$$

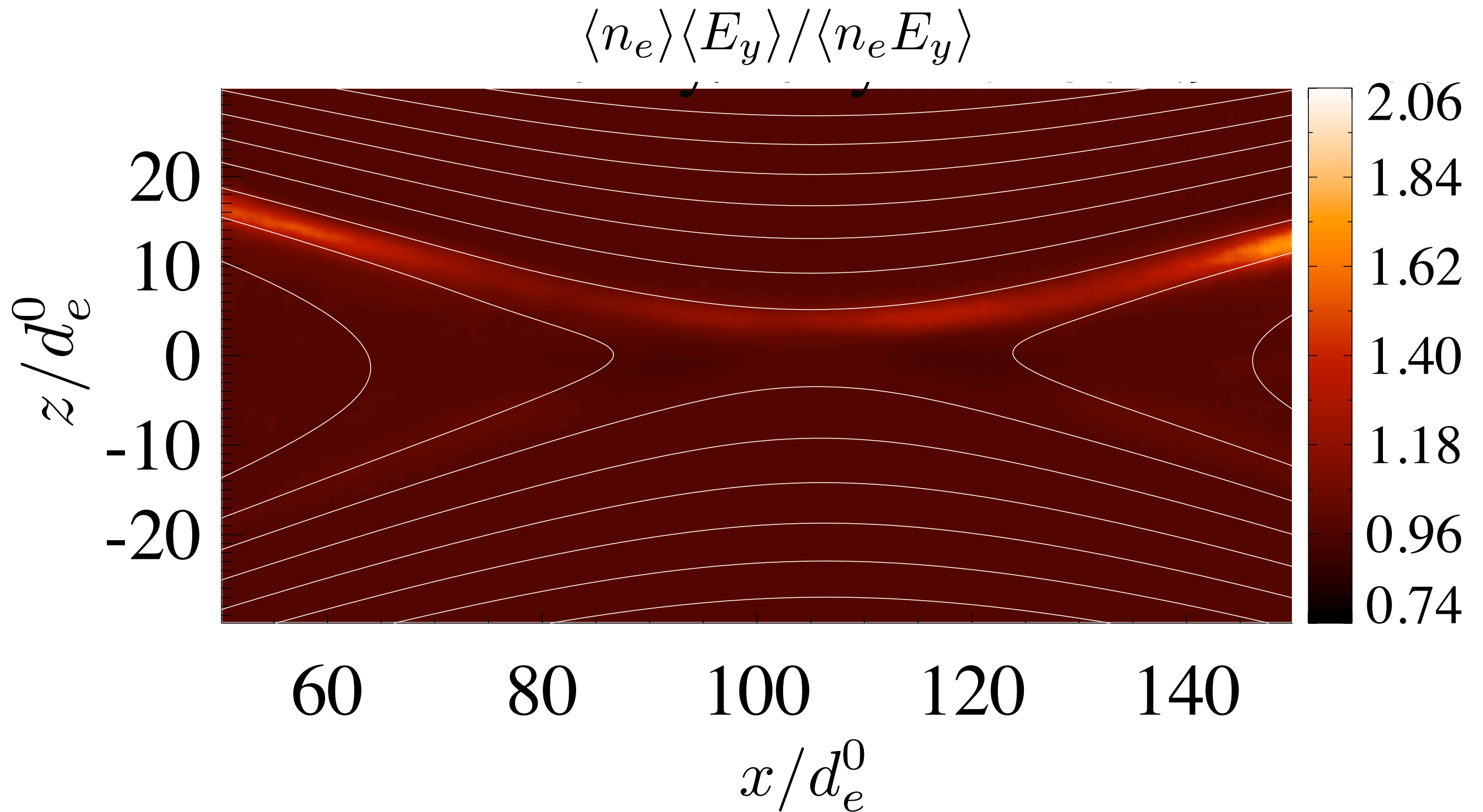
Two largest terms:

$\widetilde{\langle nE \rangle}$  induces electron-ion momentum exchange. Localized away from the X-line

$\frac{1}{c} \widetilde{\langle n(\mathbf{v} \times \mathbf{B})_y \rangle}$  describes momentum re-distribution across the layer due to kinking



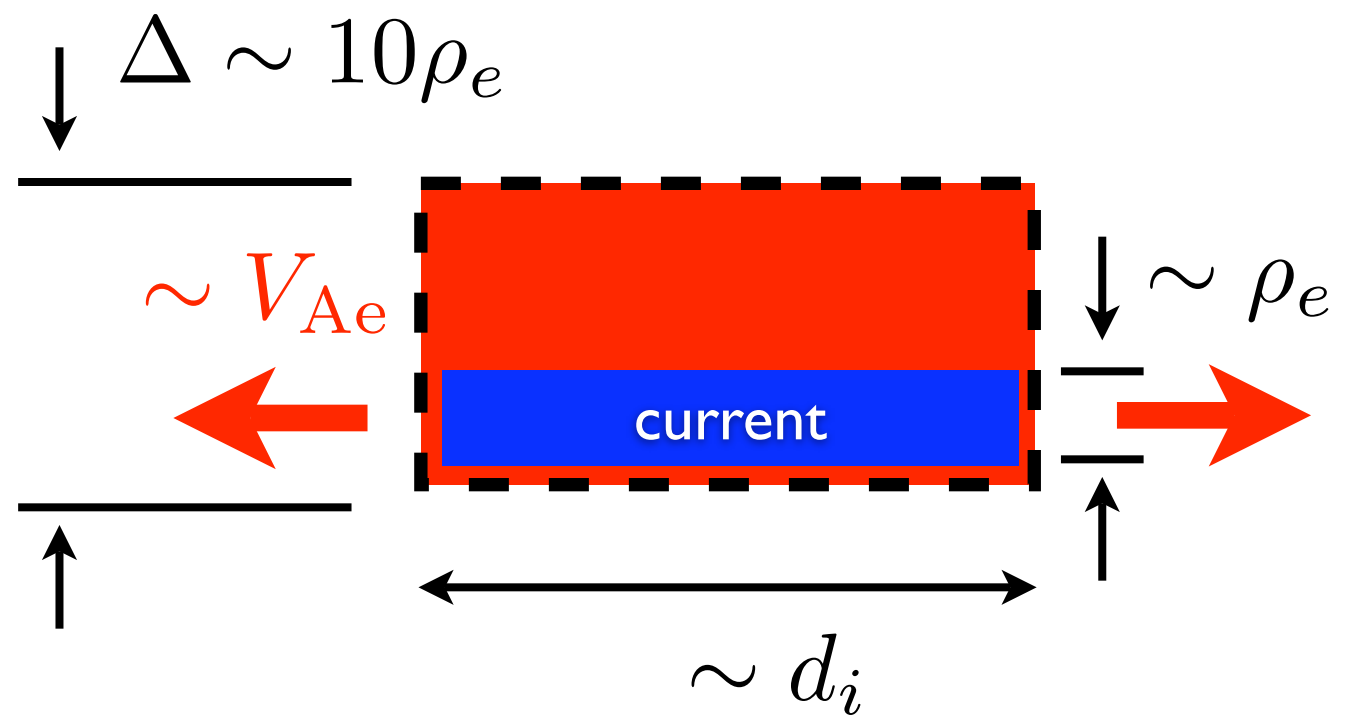
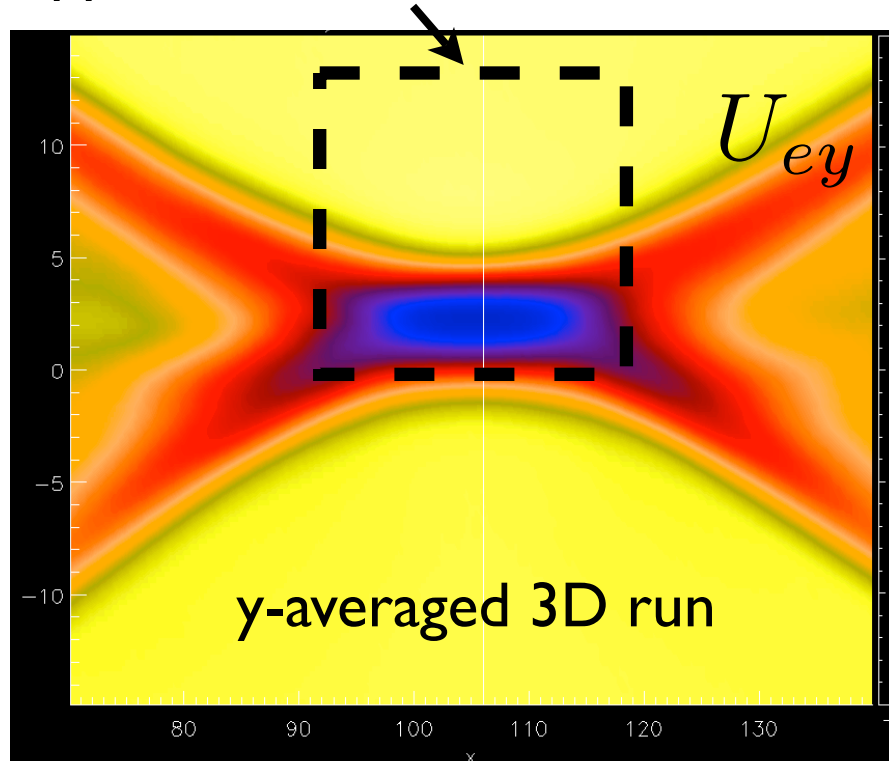
## Fluctuations are strong along the separatrices



Asymmetric configuration,  $(10 \times 10 \times 10)d_i$  based on the upstream high  $n$   
Open boundary driven simulation,  $m_i/m_e=400$ ,  $810^3$  cells,  $3.2 \times 10^{11}$  particles at  $t=0$

# To be relevant - instability must be faster than transit time for plasma through this region

approximate localization of the mode



The entire population in the “interaction” region is replaced on a time-scale

$$\tau \sim \frac{\Delta d_i}{\rho_e V_{Ae}} \sim 10 \Omega_{ci}^{-1} \left( \frac{m_e}{m_i} \right)^{1/2} = 10 \omega_{LH}^{-1}$$

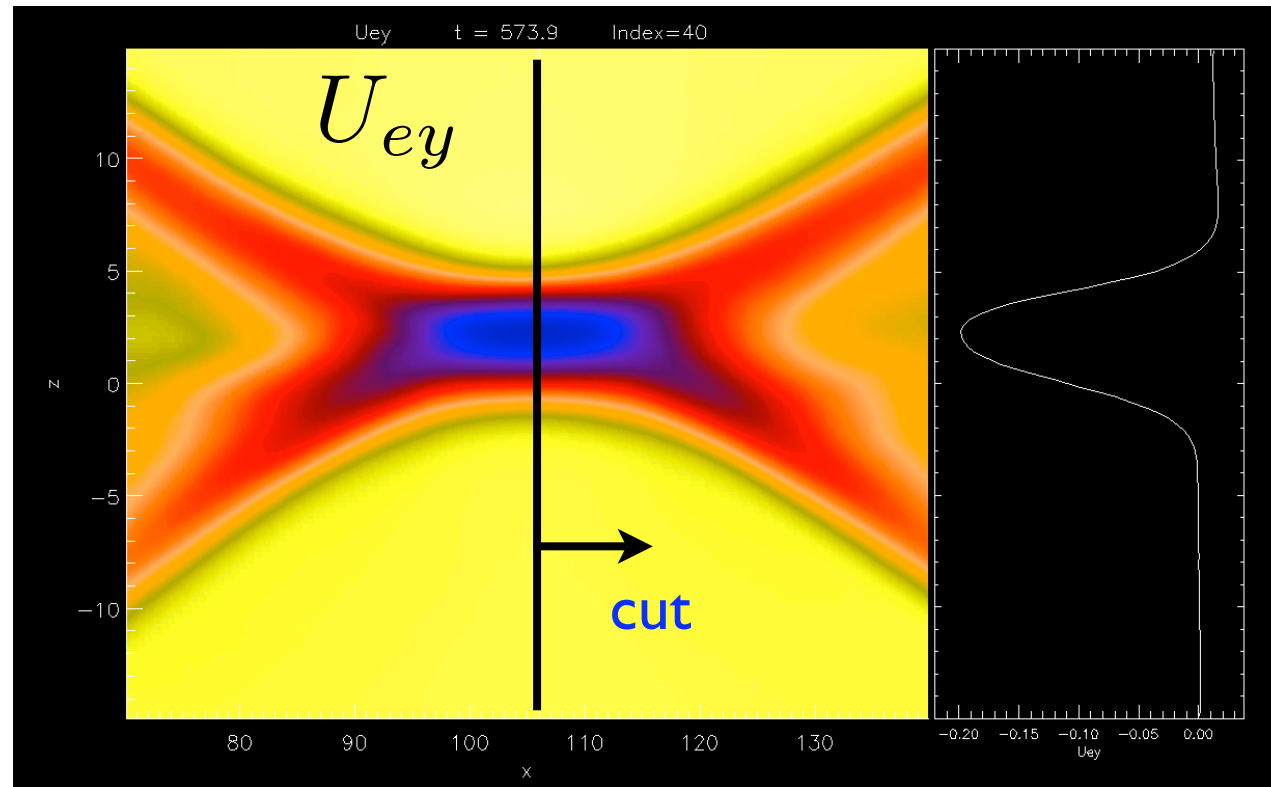
The instability can grow to large amplitude and strongly interact with particles only if  $\gamma\tau > 1$

- 1) Growth rate must be a large fraction of the lower-hybrid frequency
- 2) Instability may be stronger in elongated layers (larger  $\tau$ ) - to investigate this, need larger system

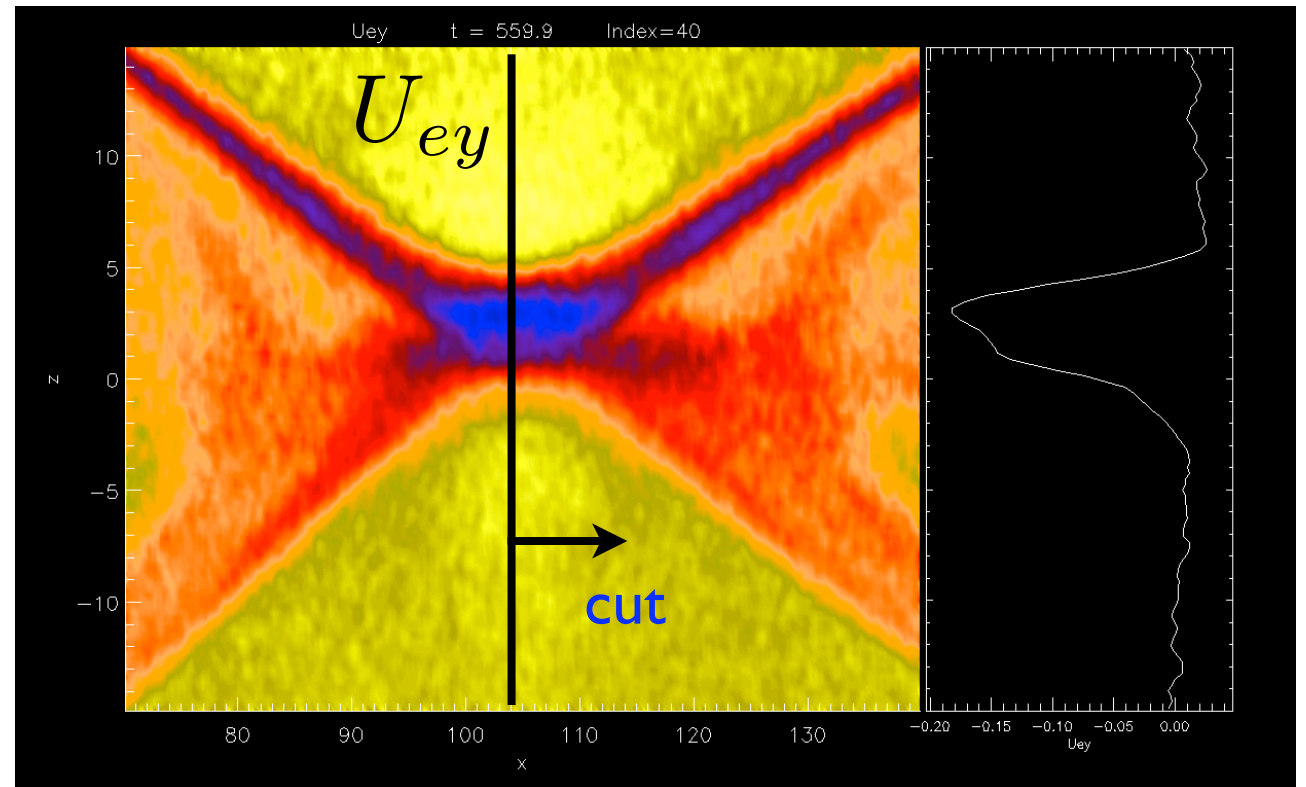
# The layer structure remains similar to corresponding 2D case

---

y-averaged 3D run



2D run



There is a tendency for layers to be longer in 3D simulations. This may become important in larger systems  
(the size of this simulation is  $< 10 d_i$  in the outflow direction)

# Summary & Future Outlook

- For 3D reconnection geometries, contributions from anomalous drag are small near the x-line, but anomalous transport is larger
- Along separatrices, there is strong anomalous drag, and this potentially could influence the global evolution
- As another interesting possibility, there is some evidence that these instabilities may seed the formation of flux ropes in 3D

